HYDROLOGIC AND ECOLOGICAL EFFECTS OF WATERSHED URBANIZATION: IMPLICATION FOR WATERSHED MANAGEMENT IN HILLSLOPE REGIONS

A Dissertation

by

CHAN YONG SUNG

Submitted to the Office of Graduate Studies of
Texas A&M University
in partial fulfillment of the requirements for the degree of

DOCTOR OF PHILOSOPHY

May 2010

Major Subject: Urban and Regional Sciences

HYDROLOGIC AND ECOLOGICAL EFFECTS OF WATERSHED URBANIZATION: IMPLICATION FOR WATERSHED MANAGEMENT IN HILLSLOPE REGIONS

A Dissertation

by

CHAN YONG SUNG

Submitted to the Office of Graduate Studies of
Texas A&M University
in partial fulfillment of the requirements for the degree of

DOCTOR OF PHILOSOPHY

Approved by:

Chair of Committee,	Ming-Han Li
Committee Members,	George O. Rogers
	Astrid Volder
	Zhifang Wang
Head of Department,	Forster Ndubisi

May 2010

Major Subject: Urban and Regional Sciences

ABSTRACT

Hydrologic and Ecological Effects of Watershed Urbanization: Implication for Watershed Management in Hillslope Regions.

(May 2010)

Chan Yong Sung, B.E., Hongik University; M.E., Hongik University;

M.P.A/M.S., Indiana University

Chair of Advisory Committee: Dr. Ming-Han Li

In this study, I examined the effect of watershed urbanization on the invasion of alien woody species in riparian forests. This study was conducted in three major steps: 1) estimating the degree of watershed urbanization using impervious surface maps extracted from remote sensing images; 2) examining the effect of urbanization on hydrologic regime; and 3) investigating a relationship between watershed urbanization and ecosystem invasibility of a riparian forest.

I studied twelve riparian forests along urban-rural gradients in Austin, Texas. Hydrologic regimes were quantified by transfer function (TF) models using four-year daily rainfall-streamflow data in two study periods (10/1988-09/1992 and 10/2004-09/2008) between which Austin had experienced rapid urbanization. For each study period, an impervious surface map was generated from Landsat TM image by a support vector machine (SVM) with pairwise coupling. SVM more accurately estimated

impervious surface than other subpixel mapping methods. Ecosystem invasibilities were assessed by relative alien cover (RAC) of riparian woody species communities.

The results showed that the effects of urbanization differ by hydrogeologic conditions. Of the study watersheds, seven located in a hillslope region experienced the diminishing peakflows between the two study periods, which are contrary to current urban hydrologic model. I attributed the decreased peakflows to land grading that transformed a hillslope into a stair-stepped landscape. In the rest of the watersheds, peakflow diminished between the two study periods perhaps due to the decrease in stormwater infiltration and groundwater pumpage that lowered groundwater level. In both types of watersheds, streamflow rising during a storm event more quickly receded as watershed became more urbanized.

This study found a positive relationship between RAC and watershed impervious surface percentage. RAC was also significantly related to flow recession and canopy gap percentages, both of which are indicators of hydrologic disturbance. These results suggest that urbanization facilitated the invasion of alien species in riparian forests by intensifying hydrologic disturbance.

The effects of urbanization on ecosystems are complex and vary by local hydrologeologic conditions. These results imply that protection of urban ecosystems should be based on a comprehensive and large-scale management plan.

ACKNOWLEDGEMENTS

I would like to thank my doctoral committee chair, Dr. Ming-Han Li, for his constant guidance and support during my graduate studies at Texas A&M University. I also would like to thank my doctoral committee members, Dr. George Rogers, Dr. Astrid Volder, and Dr. Zhifang Wang, for all the support and knowledge that they have provided me. I also would like to thank my friends for all of the casual discussions about this research. I also would like to thank my coworkers in the Texas Transportation Institute for sharing their experience and providing financial support. This study is supported by the Texas Water Resource Institute (TWRI) Mills Scholarship. Finally, I would like to thank to my parents and sister for their constant support and motivation throughout my entire life.

TABLE OF CONTENTS

LIST OF FIGURES

FIGURE Page

LIST OF TABLES

CHAPTER I

INTRODUCTION

Background

Riparian forests buffer harmful effects from surrounding areas (Basnyat et al., 2000; Groffman et al., 2002; Mitsch and Gosselink, 2007). They protect water quality of adjacent streams by filtering various types of pollutants from stormwater runoff. The filtered pollutants are stored in soil and biomass or degraded by soil microorganisms. For instance, denitrification process in riparian soils significantly removes nitrogen and consequently reduces eutrophication in downstream ecosystems (Mitsch et al., 2000; Watts and Seitzinger, 2000). A field measurement by Pinay et al. (1995) showed that riparian forests return terrestrial nitrogen to the atmosphere at the rate of 29.5 N g m^{-2} yr^{-1}.

In addition to the buffer effect, riparian forests play an important role in both global and local ecosystems. Riparian forests mitigate climate change by sequestrating a large amount of carbon in soil and biomass (Brinson, 1981). Riparian vegetation also prevents soil erosion from stream banks. Beeson and Doyle (1995) found that stream banks without vegetation eroded sediment 30 times higher than those with vegetation. Hession et al. (2003) also reported that stream channels with riparian forests are wider than the ones without forests, suggesting that vegetation reduced stream bank erosion.

This dissertation follows the style of Landscape and Urban Planning.

Urbanization threatens these valuable ecosystem services. Impervious surface along with an engineered drainage system quickly discharges stormwater into downstream and increases the frequency and magnitude of floods (Arnold and Gibbons, 1996; Burges et al., 1998; Leopold, 1968; Kim et al., 2002; Booth et al., 2004; Rogers and DeFee II, 2005; Walsh et al., 2005). The increased stormwater runoff also degrades stream water quality by washing off pollutants generated by urban activities (Barrett et al., 1998; Barbec et al., 2002; Brezonik and Stadelmann, 2002; Hatt et al., 2004; Goonetilleke et al., 2005; Schoonover et al., 2005; Alberti et al., 2007; Li et al., 2008) and by increasing soil erosion (Chin and Gregory, 2001; Jones et al., 2000). During non-storm periods, urban streams may have lower baseflow because impervious surface impedes the infiltration of stormwater (Groffman et al., 2003; Brandes et al., 2005; Meyer, 2005). The decreased stormwater infiltration lowers the groundwater table, and results in hydrologic drought in downstream and riparian ecosystems. Therefore, urban riparian forests suffer from severe disturbance regimes with higher peak discharge, degraded water quality, and drought during non-storm events.

Previous studies suggested that the increases in disturbance levels facilitate the invasion of alien species in urban riparian forests (Tickner et al., 2001; Zedler and Kercher, 2004; Burton et al, 2005; Maskell et al., 2006). Riparian ecosystems are often regulated in early successional stage because severe disturbances, especially floods, kill mature trees (Cronk and Fennessy, 2001; Pettit and Froend, 2001; Shafroth et al., 2002; Corbacho et al., 2003; Lytle and Merritt, 2004). Once floods recede, canopy gaps are quickly filled by new seedlings that consist of both native and alien species (Bendix and

Hupp, 2000; Cooper et al., 2003). However, some alien species are known to outcompete the native ones in the regenerating cohort due to their abilities to grow faster and be tolerant to disturbance (Stromberg, 1998; Vandesande et al., 2001; Morris, et al., 2002; Pratt and Black, 2006). Stream channel serves as a conduit for propagules of alien species. This implies that the invasion of alien species is not limited to urban areas, but spreads to riparian forests in downstream (Moggridge et al., 2009). The biological invasion in riparian forests is of a particular concern in arid- and semi-arid regions where the riparian forests provide irreplaceable habitats for regionally rare wetland species (Aguiar and Ferreira, 2005). Hence, increasing the invasion of alien species in riparian forests threatens regional biodiversity in this climatic region.

Research Objectives and Significance

The main objective of this study is to examine the effect of watershed urbanization on ecosystem invasibility of twelve riparian forests along urban-rural gradients in Austin, Texas. I answered this question by taking three main steps: 1) measuring the degrees of watershed urbanization; 2) examining the effect of urbanization on hydrologic disturbance regime, and 3) exploring relationships among watershed urbanization, hydrologic disturbance regime, and ecosystem invasibility of a riparian forest. Each step requires a lengthy technical description and has its own research significance that deserves to be discussed in detail. Thus, I described these tasks in three separate chapters, each of which has an introduction and conclusion.

Chapter II discussed the method of estimating the degrees of urbanization in study watersheds. I measured the degrees of urbanization using impervious surface maps generated from remote sensing images. One of the problems of using remote sensing images to extract urban land cover is that the images cannot capture the heterogeneity of urban landscape within instantaneous field of views (IFOV), i.e., more than one type of land cover occurs in a single image pixel (Small, 2001; 2002). To overcome this problem, I employed a subpixel image classification method – an image classification method that estimates the proportion of impervious surface in each pixel (Huang and Townshend, 2003; Lee and Lathrop, 2006). Of many subpixel methods, I used support vector machine (SVM) with pairwise coupling due to its ability to avoid an overfitting problem (Burges, 1998). In spite of its promising feature, it has yet been evaluated in remote sensing context. Therefore, in Chapter II, I assessed the applicability of SVM to subpixel impervious surface mapping.

Chapter III examined the effect of urbanization on stream hydrology. The effect of urbanization was examined by comparing hydrologic regimes of the same watershed before and after urbanization. I introduced the transfer function (TF) model to quantify hydrologic regimes (Young, 2003). TF models were estimated by four-year daily rainfall and streamflow data in two study periods spanning 20 years. Chapter III also discussed the factors that led to the different hydrologic consequences in two hydrogeologic regions: a gentle slope region and a hillslope region.

Chapter IV addressed a question whether and how urbanization facilitates the invasion of alien species in riparian forests. Although many studies have reported that

urban riparian forests have more alien species than rural ones (King and Buckney, 2000; Burton and Samuelson, 2008; Oneal and Rottenberry, 2008), only few directly related the hydrologic disturbance regime to the ecosystem invasibility in urban riparian forests. Lack of such study may be due to the difficulty in quantifying hydrologic regime. As discussed in Chapter III, this problem can be solved by the TF model. I also measured other environmental variables that may affect the ecosystem invasibility, including the degrees of watershed urbanization (done in Chapter II), soil nutrient contents, and vegetation community structures. Using these dataset, I explored a model that can describe a causal relationship between watershed urbanization and the invasion of alien species in a riparian forest.

Finally, I summarized the findings of three independent studies in Chapter V. I also discussed implications for urban planners and water resources and ecosystem managers.

CHAPTER II

SUBPIXEL IMPERVIOUS SURFACE MAPPING USING SUPPORT VECTOR MACHINE WITH PAIRWISE COUPLING

Chapter Summary

We evaluated the performance of support vector machine (SVM) with a pairwise coupling algorithm on subpixel impervious surface mapping, and compared SVM's performance with that of linear spectral mixture analysis (LSMA) and multi-layer perceptron (MLP). Landsat TM images of Austin, Texas taken in February and October 2008 were used to assess the three subpixel methods. The results indicate that SVM had higher estimation accuracies than LSMA and MLP. Non-linear kernel function and the structural risk minimization scheme equally contributed to the superiority of SVM to LSMA. The analysis of error shows that MLP was more appropriate for hard (per-pixel) classification. It was not effective in reflecting the variation of impervious surface in subpixel level. Comparison of the estimation accuracies by season suggests that the February image taken when tree lost foliage generated more accurate maps than the October one when lush tree canopies still existed. The low accuracy of the October image may be due to impervious surface under tree canopy that was not detectable when trees have foliage. Our results suggest 1) that SVM is suited to map impervious surface in subpixel level, and 2) that winter images generate more accurate impervious surface maps especially for urban areas in a subtropical climate.

Introduction

Impervious surface adversely affects urban environment. Stormwater runoff generated from impervious surface increases the frequency and magnitude of flood in urban streams (Arnold and Gibbons, 1996; Brabec et al., 2002; Walsh et al., 2005). Pollutants washed off from impervious surface degrade water quality of the streams (Brezonik and Stadelmann, 2002; Goonetilleke et al., 2005; Li et al., 2008). The effect of impervious surface is not limited to the urban stream. The flashy hydrology and degraded water quality further deteriorate the health of aquatic and riparian ecosystems. Many studies showed that the impervious surface alters the population density and the community structure of benthic macroinvertebrates (Gillies et al., 2003; Morse et al., 2003), fish (Wang et al., 2001; Sutherland et al., 2002), amphibian and reptile (Riley et al., 2005], and riparian vegetation (Moffatt, et al., 2004; Maskell et al., 2006).

Remote sensing images have been widely used to map impervious surfaces in urban areas. One of the problems associated with using these images is the so-called a mixed pixel problem. Urban images are covered by various surface materials within the sensor's instantaneous field of view (IFOV). Hard image classification methods – image processing methods designed to assign one class membership per pixel – cannot account for the heterogeneity in subpixel level (Fisher and Pathirana, 1990; Small, 2001; 2002).

To overcome this problem, several soft classification methods, or subpixel estimation methods, have been developed. The most common method is linear spectral mixture analysis (LSMA) that models the spectral characteristics of a pixel by a linear combination of spectrally pure pixels, namely endmembers. Ridd (1995) proposed the

vegetation-impervious surface-soil (V-I-S) model that unmixes the urban land covers with these three basic types of land covers. Later works improved Ridd's model by elaborating endmember selection schemes (Wu and Murray, 2003; Lu and Weng, 2004). Although LSMA is simple and has produced reasonably accurate subpixel maps, LSMA has some drawbacks: the spectral characteristics are not mixed linearly; and the endmembers do not always correctly represent physical surface materials (Huang and Townshend, 2003; Walton, 2008).

Many non-linear subpixel methods, such as regression trees (Huang and Townshend, 2003) and artificial neural network (ANN) (Moody et al, 1996; Liu and Wu, 2005; Lee and Lathrop; 2006) have been used to extract land cover maps from remote sensing images. However, the nonlinear methods are often overfitted and thereby sensitive to the selection of training pixels. Recently, support vector machine (SVM), a binary classification method based on statistical learning theory, has become popular due to its capacity to minimize the overfitting problem (Burges, 1998; Foody and Mathur, 2004). Previous studies have reported that SVM was very successful in land cover mapping using remote sensing images. Using this method, Nemmour and Chibani (Nemmour and Chibani, 2006) accurately detected the land cover change in Algerian capital using Landsat MSS images, and Liu et al. (2006) identified forests infested by Sudden Oak Death disease in California from data acquisition and registration (ADAR) 5500 images. SVM has also been applied to the processing of hyperspectral (Melgani and Bruzzone, 2004; Pal and Mather; 2004), synthetic aperture radar (SAR) (Lardeux et

al., 2009), and Terra multi-angle imaging spectroradiometer (MISR) images (Mazzoni et al., 2007; Su et al, 2007).

Although SVM was originally developed for hard image classification, it can extend to subpixel mapping by integrating a pairwise coupling algorithm developed by Hastie and Tibshirani (1998) and Wu et al. (2004). The basic idea of this algorithm is to estimate a probability that a pixel belongs to one land cover class from the pairwise probabilities of two land covers. The estimated probability for a land cover can directly be interpreted to the proportion of area occupied by the land cover within IFOV.

In this chapter, we compared the SVM with pairwise coupling algorithm to two commonly used subpixel methods: LSMA and multi-layer perceptron (MLP) using Landsat TM images of Austin, Texas taken in two different seasons (February and October) that represent nearly minimum and maximum tree foliage conditions, respectively. We also discussed the effect of plant phenology on the performances of the three subpixel methods.

Subpixel Estimation Techniques

Linear spectral mixture analysis

LSMA unmixes the spectral characteristics of a pixel using those characteristics of endmembers (Wu and Murray, 2003; Lu and Weng, 2004). For a pixel, the spectral characteristics, x_k, can be expressed as:

$$x_k = \sum_{l=1}^{L} p_l \, x_{k,l} + \varepsilon_k \tag{2.1}$$

where, p_l is the proportion of area occupied by land cover *l* within IFOV, L is the total number of land cover, $x_{k,l}$ is the spectral characteristics of a endmember representing land cover *l* for band *k*, and ε_k is the error of band *k*. p_l can be solved by minimizing the sum of squared errors for all bands, subject to two constraints, $\sum_{l=1}^{L} p_l = 1$ and $p_l \geq 0 \; \forall \; l$. The accuracy of LSMA largely depends on the selection of endmembers. Suitable endmembers must lie on the edge on the spectral scatterplots.

Multi-layer perceptron

MLP is one of classification methods in ANN family that feeds-forward the input data to output class membership through a network with several layers. Each layer consists of a number of nodes that resemble neurons in a biological nervous system (Moody et al., 1996; Liu and Wu, 2005). The most common structure of MLP is a three-layered network with one input, one hidden, and one output layers (Hu and Weng, 2009). Input and output nodes represent input data and output class, i.e., the numbers of input and output nodes are equal to the number of band of a sensor and the number of land cover classes, respectively. Hidden nodes receive input signals, transform, and transfer them to the output nodes. At each hidden node, the input data were transformed by the following equation:

$$h_i = f_1\left(\sum_{i=1}^{K} w_{ki} x_k\right) \tag{2.2}$$

where w_{ki} is the weight of the connection between input node *k* and hidden node *i*, K is the total number of input nodes, and f_1 is an activation function of the hidden layer. h_i is an activation value at the hidden node *i*. In a same manner, an activation value for the output node, o_l, can be calculated by:

$$o_l = f_2\left(\sum_{i=1}^{H} w_{il} h_i\right) \tag{2.3}$$

where w_{il} is the weight for the connection between hidden node *i* and output node *l*, H is the total number of hidden nodes, and f_2 is the activation function of the output layer. H is a user-specific parameter determined by trials and errors. Using training pixels, the weights, w_{ki} and w_{il}, are estimated by a back-propagation algorithm. For hard image classification, a class membership is assigned to the one with the highest o_l at the output layer. For subpixel mapping, o_l can be interpreted as the proportion of the land cover *l* within IFOV (Lee and Lathrop, 2006; Weng and Hu, 2008). After several trials, however, we recognized that existing activation functions, e.g., sigmoidal and hyperbolic tangent functions could not capture the varying degrees of impervious surface in subpixel level. Because the existing functions were designed for hard classification, output values from these functions were clustered into two extremes, i.e., close to either 0 or 1. Therefore, we used a linear activation function for f_2 and then rescaled o_ls to 0 to

1 by $p_l = o_l/(\sum_{i=1}^{L} o_l)$ where p_l is the proportion of area occupied by land cover *l* within IFOV. For f_1, we used the sigmoidal function. MLP were trained using AMORE package in R (Limas et al., 2009).

Support vector machine with pairwise coupling

SVM is a binary classifier that determines the class membership of a pixel using a separating hyperplane in feature space. The optimum hyperplane is the one with the largest margin between the data on the boundary of two classes. The data defining the margin width are called support vectors. Statistical learning theory shows that maximizing the margin width, a.k.a. structural risk minimization, can also minimize risk of overfitting by a classifier (Burges, 1998). The separating hyperplane, $f(x) = \mathbf{w} \cdot \mathbf{x} + b$, can be estimated by:

$$\min \left[\frac{\|\mathbf{w}\|^2}{2} + C \sum_{\mathrm{i}} \xi_i \right]$$

$$\text{subject to } y_{\mathrm{i}}(\mathbf{wx} + b) \geq 1 - \xi_i \text{ and } \xi_i \geq 0, \ \forall i \tag{2.4}$$

where $\mathbf{w}$ is normal to the hyperplane $f(\mathbf{x})$ and b is the bias of $f(\mathbf{x})$, respectively, ξ_i is a slack variable for a pixel *i* that is not separable by $f(\mathbf{x})$, C is a user defined parameter that penalizes ξ_i, $y_{\mathrm{i}} \in \{-1, 1\}$ which indicates the binary class membership of a pixel *i*. Using Lagrange multiplier, $f(x)$ can be written:

$$f(\mathbf{x}) = \sum_{\mathrm{i}=1}^{S} \alpha_{\mathrm{i}}\, y_{\mathrm{i}} \mathbf{x}_{\mathrm{i}} \mathbf{x}_{\mathrm{j}} + b \tag{2.5}$$

where α_{i} is a Lagrange multiplier satisfying $0 < \alpha_{\mathrm{i}} < C$ and S is the number of support vectors. SVM can extend to the non-linear classifier by replacing the dot product $\mathbf{x}_{\mathrm{i}}\mathbf{x}_{\mathrm{j}}$ in Eq. (2.5) by kernel function which implicitly maps the data into a higher dimensional feature space. The most common form of the kernel function is:

$$\mathrm{k}\left(\mathbf{x}_{\mathrm{i}}\mathbf{x}_{\mathrm{j}}\right) = \mathrm{e}^{-\gamma|(\mathbf{x}-\mathbf{x}_{\mathrm{i}})|} \tag{2.6}$$

where, γ is a parameter defined by users.

For hard classification, the class membership is determined by evaluating the sign of Eq. (2.5). For subpixel mapping, however, we need one more step. Pairwise coupling is an algorithm for estimating p_{i} given the pairwise probabilities $r_{lm,i} = \mathrm{Prob}(y_i = l \,|y_i = l \text{ or } m,\ \mathbf{x})$, where p_{i} is a posterior probability for a pixel classified to land cover l. $r_{lm,i}$ can be estimated by:

$$r_{lm,i} = \frac{1}{1 + \mathrm{e}^{A\hat{f}_i + B}} \tag{2.7}$$

where, $\widehat{f_l}$ is the decision value calculated by Eq. (2.5), and *A* and *B* are parameter to be estimated by minimizing a negative log likelihood function using five-fold cross-validation of training pixels. Since $r_{ml,i}\, p_{l,i} = r_{lm,i}\, p_{m,i}$, p_i can be estimated by:

$$\min \sum_{l=1}^{L} \sum_{m \neq l} \left(r_{ml,i}\, p_{l,i} - r_{lm,i} p_{m,i} \right)^2$$

$$\text{subject to } \sum_l^L \; p_l = 1, \text{ and } p_l \geq 0, \; \forall\, l \tag{2.8}$$

The solution of Eq. (2.8) can be found iteratively using an algorithm developed by Wu et al. (2004). p_l can be interpreted as the proportions of areas occupied by land cover class *l* within IFOV. e1071 package in R is used to train SVM with pairwise coupling (Dimitriadou et al. 2009).

Methods

Study area and images

The study area is a rectangular area (1851km^2) completely covering the City of Austin, Texas. The study area was selected because it is located above the Edwards Aquifer, a shallow karst aquifer sensitive to the contamination of surface water (Scanlon, et al., 2003). Austin is one of the most rapidly growing cities in the United States. Population increased by 62.7% in the last two decades (465 622 in 1991 to 757 688 in 2008) (U.S. Census Bureau, 2009). During the same period, impervious surface increased by 51.4%

(10.9% to 16.5%) (See Chapter III). To protect the aquifer from this rapid urban growth, it is necessary to monitor the change in impervious surface on the recharge zone of the aquifer in a timely manner.

We extracted impervious surfaces from two cloud-free Landsat TM images (band 1-5, 7) acquired on February 07 and October 20, 2008. Two images were selected so that we can evaluate the effect of plant phenology on the performance of subpixel methods. In the study area, October is still during the growing season and almost all plants have foliage. February is in the dormant season when deciduous trees have dropped their leaves. Before the subpixel mapping, two images were atmospherically corrected by FLAASH module in ENVI 4.5 (ITT Visual Information Solutions, 2008). Previous studies reported that minimum noise fraction (MNF) transformation can improve the estimation accuracy of LSMA. Our preliminary analysis also showed that MNF transformation improved the estimation accuracies not only of LSMA but also of MLP and SVM. Therefore, for fair comparison, we used six MNF component images for all three methods.

The selection of training pixels

We selected training pixels from five land cover classes: high-albedo impervious surface (e.g., cement and glass), low-albedo impervious surface (e.g., asphalt), forest, grass/agriculture (e.g., lawn and farmland), and waterbody. For each land cover class, nine to twelve polygons evenly distributed in the study area were selected. Each polygon consists of 4 to 16 pure pixels. The total number of pixels was 522, i.e., around 100

pixels per each class. The training pixels were selected by looking into 2008 aerial photographs with 0.5 m of spatial resolution. For LSMA, we used the mean values of training pixels for each class as endmembers. As shown in Fig. 2.1, the mean values roughly lie on the edge of spectral scatterplots of pairs of the first three MNF component images, except low-albedo impervious surface whose endmember is not clearly discernable and confused with waterbody and forest. We tried both a four-class (without low-albedo impervious surface) and a five-class (with low-albedo impervious surface) training options, but the five-class option was more accurate. Thus, we trained three subpixel methods using five land cover classes.

Accuracy assessment

For accuracy assessment, we measured the proportions of impervious surface for 300 reference pixels randomly selected from Landsat TM images. For each pixel, impervious surface was on-screen digitized over the 2008 aerial photographs. We initially tried to evaluate the performance of SVM on mapping high- and low-albedo impervious surfaces separately, but we recognized many impervious surface materials cannot be clearly delineated into these two classes in a real urban landscape. To avoid inaccuracy, we measured the proportions of impervious surface regardless of the reflectivity of surface materials. Accordingly, the estimated proportions of two types of impervious surfaces were summed before accuracy assessment.

One of the problems extracting impervious surface from remote sensing images is impervious surface under tree canopies (Lee and Lathrop, 2006). To test the effect of

February 07, 2008

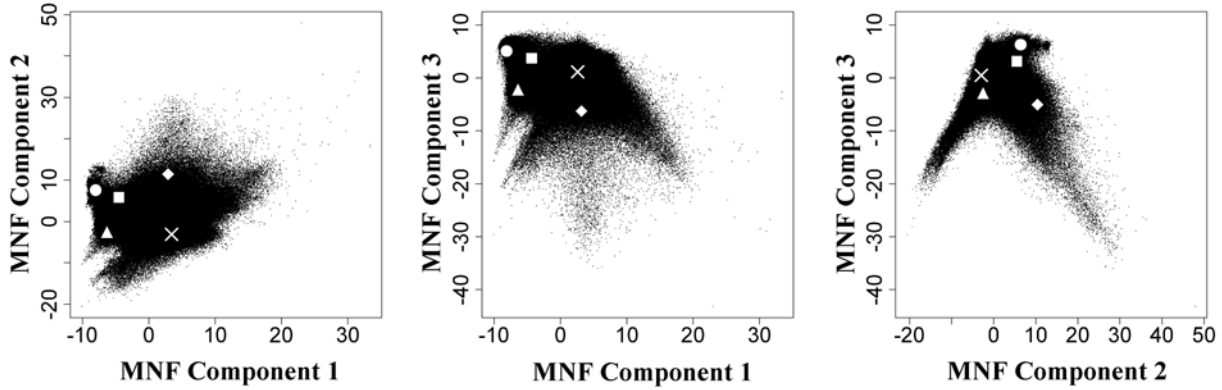

October 20, 2008

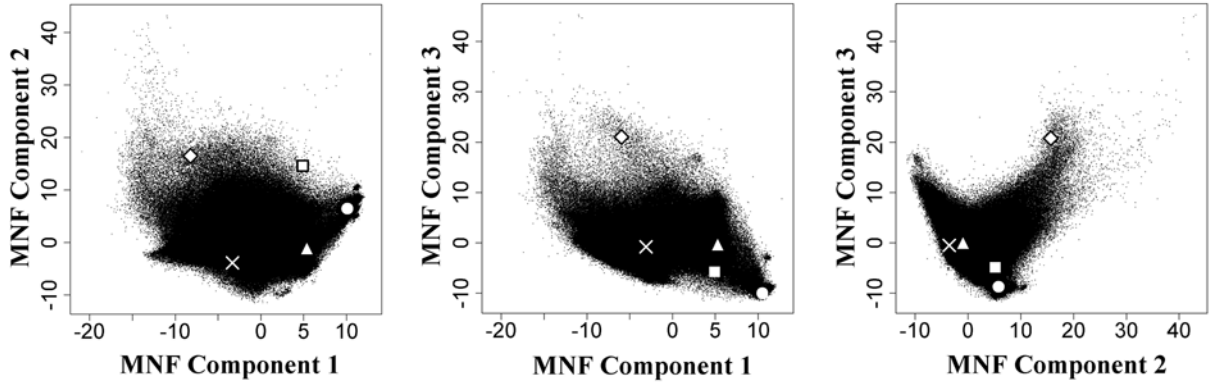

Fig. 2.1. Five endmembers on spectral scatterplots between the pairs of three MNF images (Components 1, 2, and 3). The endmembers were determined by taking the means of training pixels representing each of five land covers (◊: high-albedo impervious surface; □: low-albedo impervious surface; Δ: forest; ×: grass/agriculture; ○: waterbody).

tree canopy on the performance of SVM, we measured the proportion of impervious surface on the ground level. This procedure requires somewhat subjective decision because the actual boundary of impervious surface under tree canopy is not visible on the aerial photographs. To minimize the subjectivity in delineation, we referred to historic aerial photographs acquired during the early stage of the development when existing trees were clearcut and newly planted landscape trees were not mature. Because impervious surface may not change much over time, historic aerial photographs can provide ground cover information that may be obstructed by the tree canopy in today's aerial photographs. Four historic aerial photographs taken in 1984, 1987, 2000, and 2006 were used for referencing.

Accuracy assessments were done by calculating root mean square error (RMSE), mean absolute error (MAE), and Nash-Sutcliffe model efficiency coefficient (R^2):

$$\text{RMSE} = \sqrt{\frac{\sum_{i=1}^{N}(\hat{p}_i - p_i)^2}{N}} \tag{2.9}$$

$$\text{MAE} = \frac{\sum_{i=1}^{N}|\hat{p}_i - p_i|}{N} \tag{2.10}$$

$$R^2 = 1 - \frac{\sum_{i=1}^{N}(\hat{p}_i - p_i)^2}{\sum_{i=1}^{N}(p_i - \bar{p})^2} \tag{2.11}$$

where $\hat{p}_i$ is the estimated impervious surface proportion of reference pixel i, p_i is

Table 2.1. User specific parameters and accuracy assessments for two images (February and October) by three methods.

Methods	Parameters	R^2	RMSE	MAE
February 07, 2008				
LSMA	-	0.603	0.192	0.131
MLP	# hidden node=100	0.597	0.193	0.118
SVM	C =2960, γ =1×10^{-5}	0.663	0.177	0.116
October 20, 2008				
LSMA	-	0.442	0.228	0.155
MLP	# hidden node=50	0.384	0.239	0.150
SVM	C =850, γ =1×10^{-5}	0.500	0.215	0.146

measured impervious surface proportion of the reference pixel i, $\bar{p}$ is the mean of p_i. R^2 ranges -∞ and 1, and can be read similar to regression R^2 (Nash and Sutcliffe, 1970). The negative values only occur when the model performs very poorly. The user-specific parameters (H for MLP, and C and γ for SVM) were determined so that each method has the best estimation accuracy (Table 2.1).

Results

Fig. 2.2 illustrates subpixel land cover maps generated by SVM with pairwise coupling. SVM effectively extracted the land covers from two Landsat TM images. Major urban features, such as airport runway and major roads, are clearly identified on impervious surface maps, especially on low-albedo impervious surface maps, in both seasons. The forest and grass/agriculture maps successfully discriminate the land cover/land use in the study area, e.g., farms and ranches in the east and large forests in the west of the study area. Other geographic features, such as stream and river channels and reservoirs, are also identified on the maps.

Fig. 2.3 displays the subpixel impervious surface maps by three different methods. Again, the proportion of impervious surface in each pixel is the sum of the proportions of high- and low-albedo impervious surfaces. All maps look similar and major urban features can be identified. Three accuracy assessment measures provide more detailed analyses on the accuracy of subpixel mapping. For the February image, SVM estimated the impervious surfaces more accurately than other methods. R^2 was 0.663 for SVM, the highest among three methods (Table 2.1). SVM's lowest RMSE (0.177) and MAE (0.116) also indicate the lowest degree of estimation error by SVM. A comparison of LSMA and MLP suggests that two methods had similar estimation accuracies. RMSE and R^2 show a better performance of LSMA while MAE shows a better performance of MLP. For the October image, SVM had the highest accuracy for impervious surface mapping. R^2 was 0.500 for SVM while 0.442 and 0.384 for LSMA and MLP, respectively. RMSE and MAE accuracy measures also indicate that

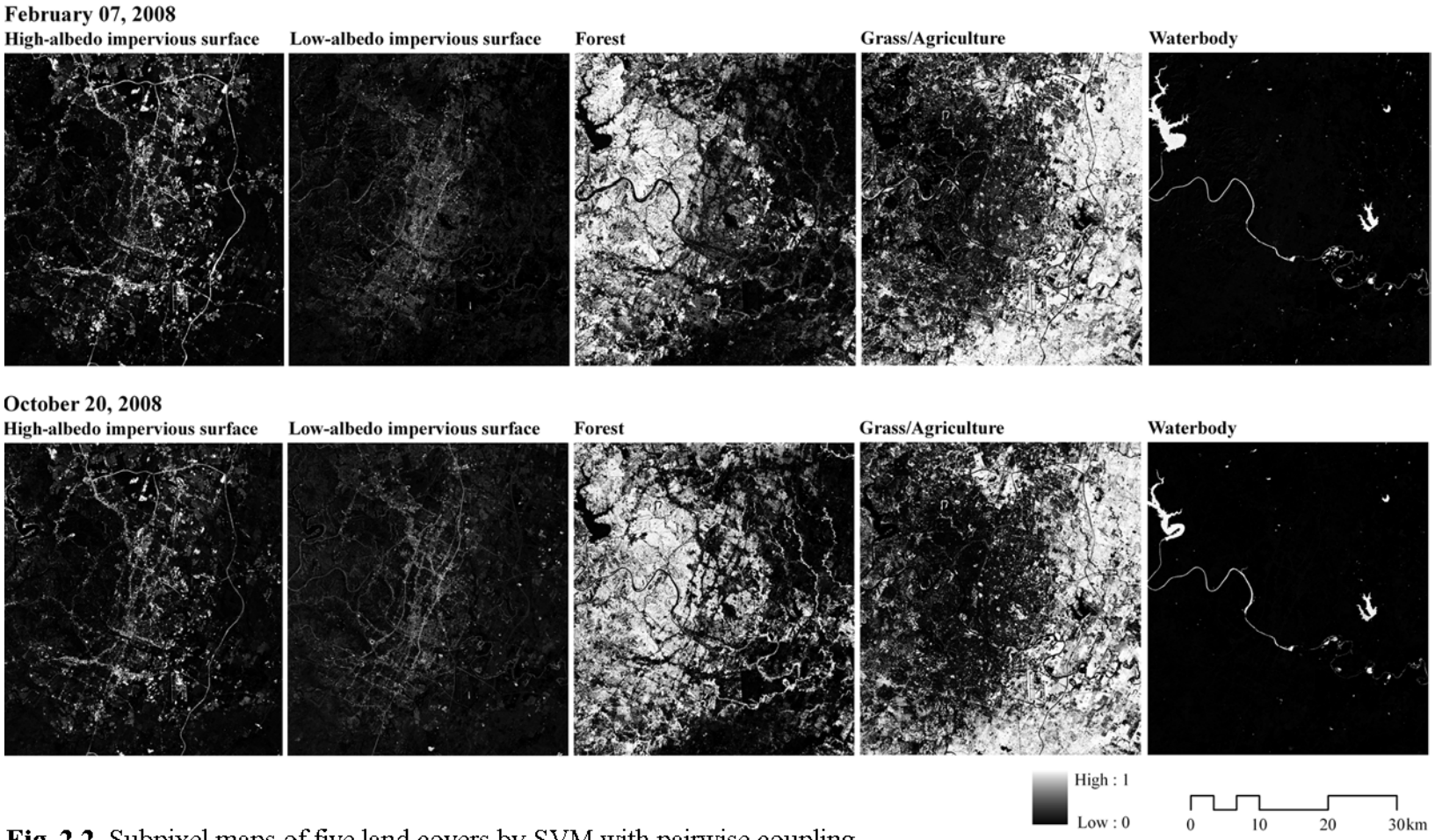

Fig. 2.2. Subpixel maps of five land covers by SVM with pairwise coupling.

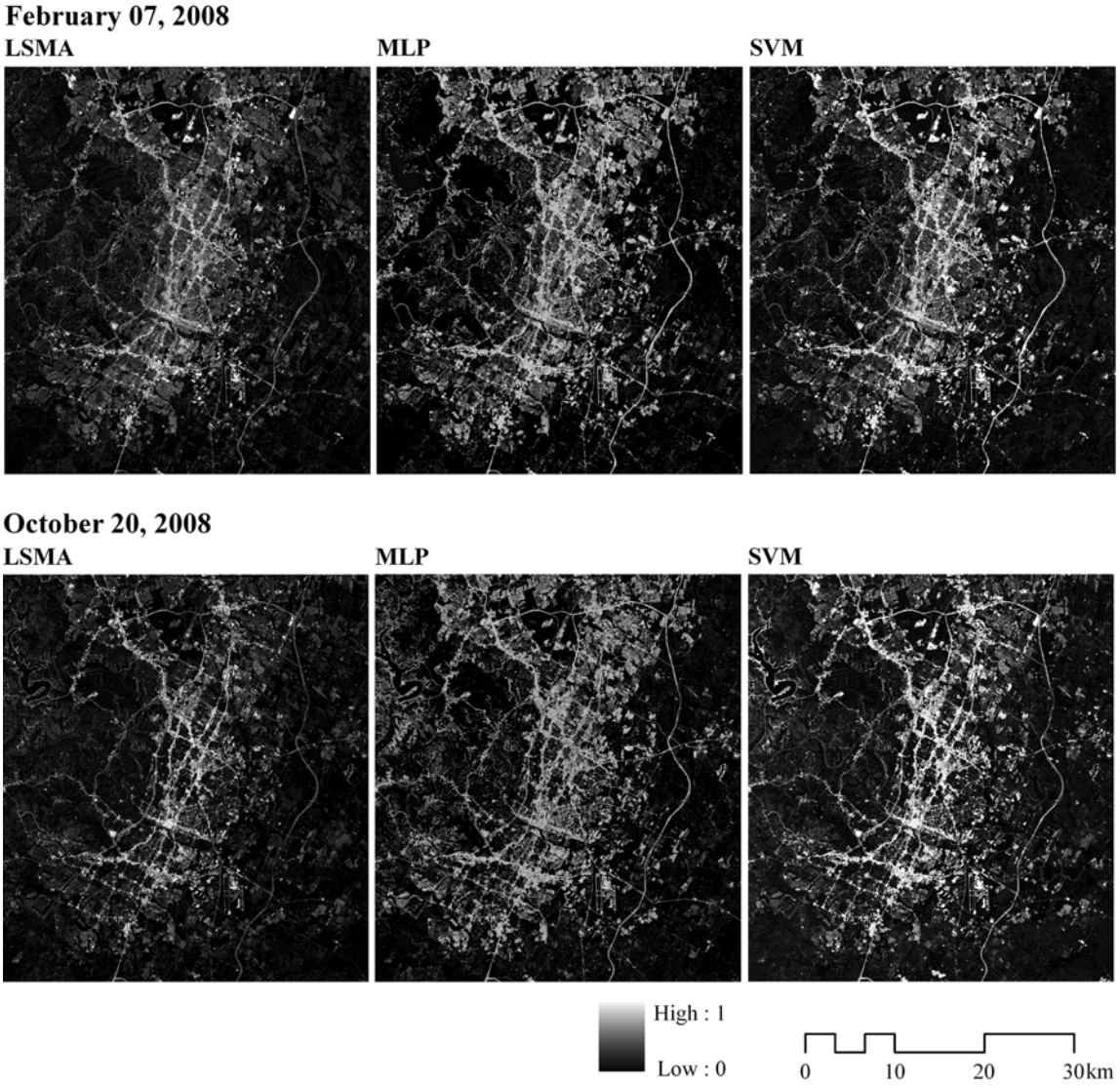

Fig. 2.3. Subpixel impervious surface maps by LSMA, MLP, and SVM.

SVM was more effective for subpixel impervious surface mapping. Like the February image, no consensus among the accuracy measures in comparison of LSMA and MLP was found and therefore, two methods can be considered similar in mapping the impervious surfaces from the October image.

Comparison on mapping accuracies of the same methods by different season shows that the February image resulted in more accurate impervious surface maps than the October image. Therefore, images of the winter season when tree dropped leaves are more suited for the subpixel mapping of the impervious surface than those of other seasons.

Discussion

The superiority of SVM to LSMA can partially be explained by confusion of low-albedo impervious surface with other land covers, particularly with waterbody (see Fig. 2.1). The inseparability of the low-albedo impervious surface has been discussed by other studies (Small, 2001; 2002). These studies indirectly solved this problem by masking out the waterbody prior to the image processing (Wu and Murray, 2003; Weng and Hu, 2008; Hu and Weng, 2009) or by employing a multi-level classification scheme (Alberti et al., 2004), but both approaches require additional time and effort. SVM bypasses this problem by introducing a kernel function that brings a non-linearity to SVM. To verify the effect of kernel function, we also conducted the same analysis but with the linear kernel function. For the February image, R^2 of SVM with the liner kernel function decreased to 0.632 (C=580), approximately in the middle of R^2s of SVM with radial

kernel (0.663) and LSMA (0.603). This result suggests that non-linear classification by the kernel function made about half of the difference between SVM and LSMA. Another half of the difference can be attributed to the structural risk minimization scheme of SVM.

The comparison of SVM and MLP suggests that MLP is not effective for subpixel mapping. Compared to SVM, MLP tended to estimate more zero percent impervious surfaces for pixels that in fact have a certain areas of impervious surfaces. This type of error is illustrated by the clouds of dots along Y-axes in Fig. 2.4 that shows the scatterplots between measured and estimated impervious surface proportions for 300 reference pixels. The density and heights of the clouds are much higher on the scatterplots for MLP than the plots for SVM, which represents greater magnitude of this type of error by MLP. Again, MLP was initially developed for hard image classification. Because the training algorithm of MLP is based on minimizing the errors between the activation values and the binary code indicating the class membership at the output nodes, the weights must be determined so that the activation values are close to 0 or 1. We tested various activation functions including softmax function, the one designed for subpixel estimation (Moody et al., 1996), but none of them showed better outcomes than our approach, i.e., applying the linear activation function and rescaling the activation values from 0 to 1. Pairwise coupling algorithm was less vulnerable to this type of error. Some studies trained MLP with continuous scale output data, i.e., with the proportions of five land cover classes (Liu and Wu, 2005). Although this approach resulted in higher accuracy, it cannot be widely applied because of the difficulty in clearly classifying

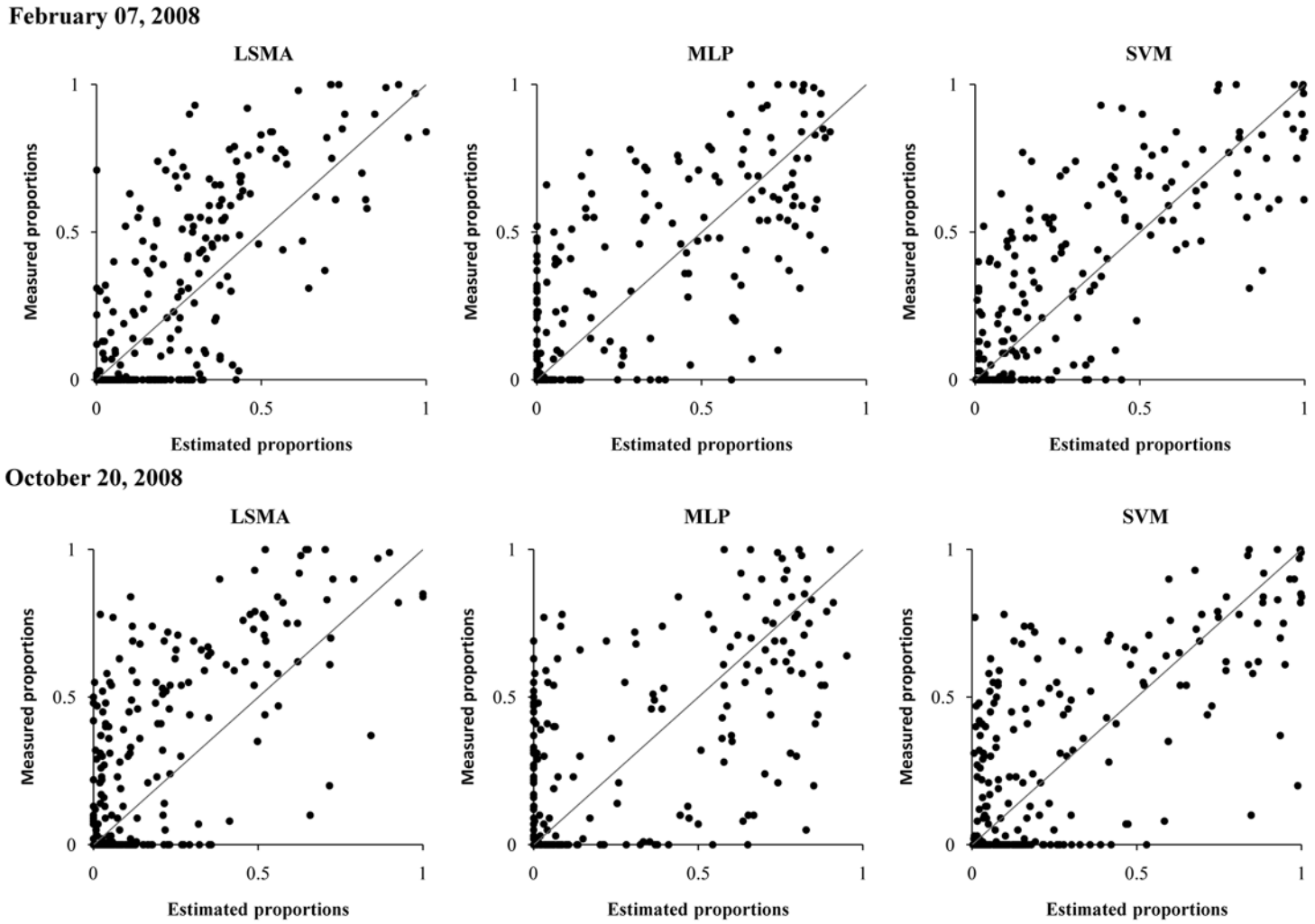

Fig. 2.4. Scatterplots between the measured and estimated proportions of impervious surfaces with 45° reference lines.

various surface materials into one of discrete land cover classes in a real urban landscape. High cost of data collection also makes this approach less practical.

Our finding suggests that a winter image is more appropriate for subpixel impervious surface mapping, which is contrary to the findings of previous studies (Weng and Hu, 2008; Hu and Weng, 2009). For instance, Hu and Weng (2009) discussed that dense foliage in summer increases the contrast between vegetation and impervious surface in Indianapolis, Indiana, and thereby results in higher estimation accuracy. The difference between this and previous studies can be explained by the difference in plant phenology. Austin's climate is subtropical and some trees and lawns remain green in winter (February). Many pixels in the winter image have a typical spectral curve of the vegetation, i.e., the abrupt change in reflectance at near infrared. Meanwhile, many trees lose foliage during winter, which allows a sensor to better detect impervious surfaces under tree canopies. The lower accuracy when using the October image can also be identified in Fig. 2.4. Comparison of the pairs of scatterplots for the same method shows that the October image had more dots along the Y-axis. This type of error suggests that impervious surface is underestimated when using the October image, perhaps due to the tree canopy that hides the impervious surfaces underneath it. Therefore, the improved accuracy of impervious surface map using the winter image can be attributed to the higher visibility below the tree canopy.

Conclusion

In this study, we compared three subpixel impervious surface mapping methods. SVM with pairwise coupling estimated the impervious surface more accurately than LSMA and MLP. Both non-linearity and the structural risk minimization scheme make SVM superior to LSMA. LSMA did not successfully discriminate low-albedo impervious surface and waterbody, suggesting that this method is not appropriate for impervious surface mapping in a region where waterbody covers a significant portion of the area. For MLP, the training algorithm specialized for hard classification leads to a lower subpixel estimation accuracy. The linear activation function mitigates this problem to some degree, but not completely. Finally, we found that the impervious surface can be more successfully extracted from the winter image in the study area due to reduced tree canopy cover.

CHAPTER III

THE EFFECT OF URBANIZATION ON STREAM HYDROLOGY IN HILLSLOPE WATERSHEDS IN CENTRAL TEXAS

Chapter Summary

This study examined the effect of urbanization on stream hydrology in hillslope watersheds. Ten streams (seven in hillslope and three in gentle slope watersheds) around Austin, Texas were selected for analysis. For each stream, we compared parameters of transfer function (TF) models estimated from daily rainfall and streamflow data collected in two study periods (10/1988-09/1992 and 10/2004-09/2008) representing different degrees of watershed urbanization. As expected, the streams became more intermittent as the watersheds were more urbanized in all the study streams. However, the effect of urbanization on peakflow differs between hillslope and gentle slope watersheds. After watershed urbanization, peakflow increased in gentle slope watersheds, but it decreased in hillslope watersheds. Based on the results of the TF models, we found that urban stream became less flashy but drier in hillslope watersheds. Overpumpage of aquifer has been recognized as a problem that leads to the stream dryness in the study area. However, the overpumpage alone cannot explain the differences in hydrologic changes between the two types of watersheds. We attributed the reduced peakflow and stream dryness in the hillslope watersheds to land grading for construction forming stair-stepped or terraced landscape. Compared with natural hillslope, a stair-stepped landscape infiltrates more stormwater by slowing down surface

runoff on tread portions of the stair. Our findings suggest that a watershed management scheme should take into account local hydrogeologic conditions to mitigate the stream dryness resulting from urbanization in hillslope watersheds.

Introduction

Urban streams suffer from flashy hydrology with frequent floods and low baseflow. Urban watersheds run off more stormwater because of increased impervious surface (Leopold, 1968; Hollis, 1975; Arnold Jr. and Gibbons, 1996; Rose and Peters, 2001; Booth et al., 2002; Burns et al., 2005; Walsh et al., 2005). Engineered drainage systems, such as stormwater sewer pipes and open channel ditches, quickly discharge the stormwater runoff from the impervious surface, and raise peakflow during a storm event much higher and quicker after watershed urbanization. Meanwhile, impervious surface also decreases baseflow during dry periods by impeding infiltration of stormwater and lowering the groundwater level (Simmons and Reynolds, 1982; Groffman et al., 2002; 2003).

There are many previous studies that have reported flashier hydrology in urban streams. Most of them were carried out in gentle slope watersheds where stormwater runoff moves slowly over the ground surface and does not seriously erode soil (e.g., Jennings and Jarnagin, 2002; Rogers and DeFee II, 2005; White and Greer, 2006). This type of watersheds generally has a soil with a deep A horizon and high water holding capacity. Paving these watersheds dramatically reduce the surface permeability and, therefore, result in flashy hydrology.

Does a similar phenomenon occur in a hillslope watershed? In hillslope watersheds, stormwater easily runs off over the steep sloped surfaces (Jackson, 1992; Wilcox et al., 2008). Because the large volume and the high velocity of the surface and subsurface flows result in severe soil erosion, the soil layers are generally shallow and bedrocks are often exposed on surface. Streamflow in these watersheds is relatively flashy even before urbanization occurs and the impact of pavement on the stream hydrology may not be as significant in hillslope as in gentle slope watersheds.

However, the effect of urbanization in hillslope watersheds is not limited to the increase in surface permeability. Land grading, a common practice for the construction of buildings on hillslope, alters local topography into stair-stepped or terraced landscape (see Fig. 3.1). This change in topography may lead to change in local hydrogeologic characteristics that cannot be predicted by conventional watershed models that are primarily based on the watershed permeability. Considering that an incorrect hydrologic prediction can result in significant damage to downstream, understanding the impact of urbanization on stream hydrology in hillslope watersheds is needed.

In this paper, we explored how urbanization alters hydrologic regime of hillslope watersheds. We studied ten streams around Austin, Texas. Of the ten streams, seven were located in hillslope watersheds and the other three in gentle slope watersheds. Transfer function (TF) models were used to quantify time series relationships, on a daily scale, between rainfall and streamflow (Salas et al., 1985). Previous studies showed that TF models successfully predicted streamflow given rainfall data (e.g., Young and Beven, 1994; Nwakalila, 2001; Young, 2003; Farahmand et al., 2007). For each stream, we

Fig. 3.1. Typical stair-stepped landscapes altered by land grading for the construction of buildings and roads in hillslope watersheds. Photographs were taken in Bull Creek (top and bottom) and Barton Creek (middle) watersheds on October 30, 2009.

estimated two TF models using rainfall-streamflow data from two study periods spanning approximately 20 years. Since the study area had experienced rapid urbanization, the comparison of model parameters for the two study periods allowed us to examine the effect of the watershed urbanization on stream hydrology.

Methods

Study area

The study area includes ten watersheds around Austin, Texas where the Blackland Prairie meet the Hill Country across the Balcones Escarpment (Fig. 3.2). The Blackland Prairie, a flat to gently rolling plain, lies on the eastern half of the study area. This region is underlain with a Houston Black soil with a deep (150 cm) and well drained clay A horizon (Soil Conservation Service, 1974). Across the Balcones Escarpment to the west is the Hill Country, the eastern border of the Edwards Plateau. In this region, topography dramatically changes to rugged landscape with rocky hills and deep valleys. The dominant soil is a Brackett soil that has a shallow (15 cm) A horizon with gravel and clay loam weathered and eroded from the underlying Cretaceous limestone bedrock (Soil Conservation Service, 1974). The bedrock consists of alternating limestone and dolomite layers interbedded with soft marly layers. As the marl is weathered and eroded, the slope fails and the upper layer recedes. This process has formed a stair-stepped landscape with a series of treads and risers (Marsh and Marsh, 1995; Woodruff Jr. and Wilding, 2008). Naturally occurring steps have a dimension of approximately 2 m in height and 10-20 m in width (Wilcox et al., 2007).

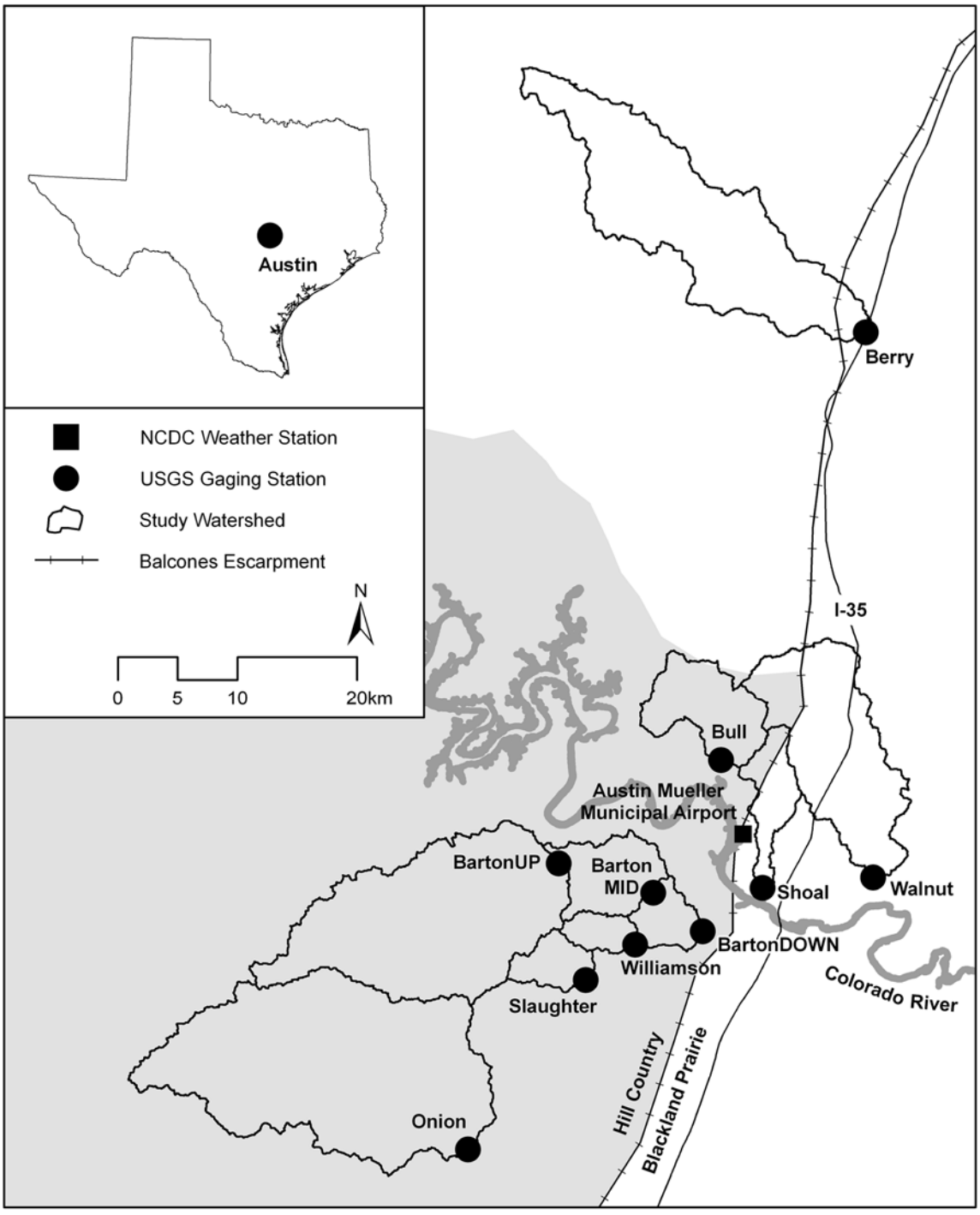

Fig. 3.2. Ten study watersheds.

The Edwards Aquifer, a shallow karst aquifer underneath the study area, plays an important role in stream hydrology. This aquifer is mainly recharged via fractures and cracks of the limestone bedrock along streambeds near the Edwards Escarpment, called the recharge zone. About 75% of aquifer recharge occurs along the streams (Bowles and Arsuffi, 1993). The aquifer also discharges to the streams from many artesian springs. Overpumpage of the Edwards Aquifer has long been a concern. Many springs have dried up as water was pumped out of the aquifer for agricultural and residential consumption over the last decades. The Colorado River, crossing the Edwards Escarpment from northwest to southeast in the study area, divides the aquifer into two sections: the Barton Springs segment and the Northern segment (Scanlon et al., 2003). The climate is subtropical with a mean annual precipitation of 810 mm falling more on spring and fall [U.S. National Climatic Data Center (NCDC), 2009]. Snow is rare.

Austin is one of the fastest growing cities in the United States. The population almost doubled over the last two decades from 465,622 in 1990 to 757,688 in 2008 (U.S. Census Bureau, 2009). Many natural and agricultural lands surrounding the city were converted to suburban areas. We selected ten intermittent streams whose watersheds cover varying degrees of urbanization from downtown to suburban and to rural areas. At each stream, the U.S. Geological Survey (USGS) has monitored daily mean streamflow for more than 20 years. Other USGS stations located at the Colorado River or whose watersheds lie in both the Blackland Prairie and the Hill Country were excluded from analysis. Table 3.1 describes the characteristics of the ten watersheds chosen for this study. Of the ten study watersheds, seven are located in the Hill Country and the

Table 3.1. Characteristics of ten USGS gaging stations and their contributing watersheds.

USGS ID	Site Name*	Area of watershed (km^2)	Mean Slope (%)	Geologic region
08158600	Walnut Creek	138.4	3.99	Blackland Prairie
08156800	Shoal Creek	33.0	3.33	Blackland Prairie
08105100	Berry Creek	213.9	2.14	Blackland Prairie
08154700	Bull Creek	58.7	11.07	Hill Country
08158920	Williamson Creek	16.3	6.35	Hill Country
08158840	Slaughter Creek	22.7	5.38	Hill Country
08155200	BartonUP Creek	231.8	6.97	Hill Country
08155240	BartonMID Creek	278.0	7.69	Hill Country
08155300	BartonDOWN Creek	301.6	7.78	Hill Country
08158700	Onion Creek	320.2	6.16	Hill Country

* The suffixes, “UP”, “MID” and “DOWN,” refer to upstream, midstream, and downstream of Barton Creek.

remaining three in the Blackland Prairie. Barton Creek is monitored by three gaging stations. Thus, the number of the streams studied is eight in total. Seven streams are tributaries of the Colorado River. Berry Creek flows into the Brazos River.

Measurement of watershed urbanization

The degree of watershed urbanization was measured by impervious surface percentage of the watershed, a commonly used indicator of urbanization (Arnold and Gibbons, 1996; Brabec et al., 2002). Two impervious surface maps were generated from cloud free Landsat TM images acquired on February 8, 1991 and February 7, 2008. Winter images were selected to more easily detect impervious surfaces under tree canopies. We

used the support vector machine (SVM) for mapping impervious surfaces because of its ability to minimize errors near the boundary between land cover classes (Burges, 1996, Foody and Mathur, 2004; 2006). This attribute is particularly promising for urban remote sensing images because urban landscape consists of diverse surface materials within an image pixel.

We classified two images separately into four land cover classes: impervious surface, forest, grassland, and waterbody. Since SVM is a supervised classification algorithm, i.e., SVM assigns each pixel into one of the land cover classes predefined by users, we trained it using 40 rectangular polygons (10 polygons per each land cover class), each of which consists of four to ten pure pixels representing each land cover. The training pixels were selected with aids of aerial photographs taken in 1987 and 2006. For impervious surface, the training pixels covered various construction materials such as concrete, cement and glass. We applied the second order polynomial kernel to non-linearly separate impervious surface from other land cover classes. We also included a slack variable to penalize errors for training pixels not separable by SVM. The weight of the slack variable, the level of penalty for the errors, was determined by trial-and-error so that SVM has the highest classification accuracy. 58 validation pixels were additionally obtained to assess the classification accuracy. Initially, we randomly selected 300 validation pixels and measured the area of impervious surface for each pixel by on-screen digitizing over the 1987 and 2006 aerial photographs. However, only 29 pixels had impervious surfaces greater than 50%. Thus, 29 non-impervious pixels were randomly selected from remaining 271 pixels. The pixels that experienced land

cover change between the two study periods were excluded from training or validation pixels. Because we are only interested in impervious surface, three non-impervious land cover classes classified by the SVM were merged into one class before assessing classification accuracy. The optimum weight for the slack variable is the one that yields the highest classification accuracy. Once impervious surface was classified, impervious surface percentages were calculated for ten watersheds delineated from 1 arc-second National Elevation Dataset. ENVI 4.5 was used for the SVM classifications (IIT Visual Information Solutions, 2008).

Transfer function model

TF models were estimated using daily rainfall and daily mean streamflow data collected in two 4-water year (WY) periods: 1989-1992WY (10/1988 to 09/1992) and 2005-2008WY (10/2004 to 09/2008). Daily rainfall data were measured at Austin Mueller Municipal Airport (NCDC COOPID: 410428) located approximately at the center of the study area. Although there were other weather stations near some of the study watersheds, we did not use the data from those stations because they did not measure the daily rainfall from midnight to midnight. Mean annual precipitations were 929 mm and 863 mm for 1989-1992WY and 2005-2008WY, respectively, both of which were higher than a long-term average (810 mm). Fig. 3.3 illustrates daily hyetograph and hydrographs for Shoal Creek (the most urbanized stream) for the two study periods. For BartonUP Creek and BartonMID Creek where the USGS had missing data during the

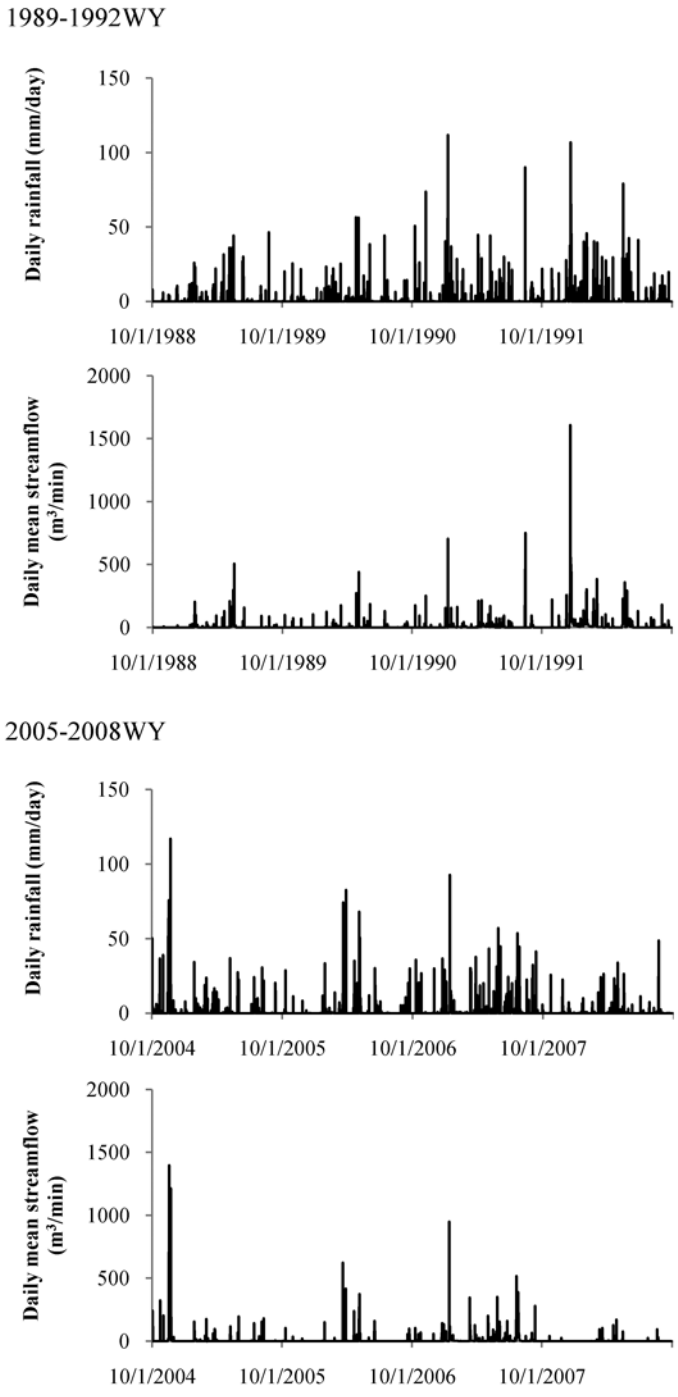

Fig 3.3. Daily hyetographs and hydrographs for two study periods. Daily rainfall depth and daily mean streamflow were measured at Austin Mueller Municipal Airport and Shoal Creek gaging station (the one flowing near downtown Austin), respectively.

first two months in 1989-1992WY period, TF models were estimated with the remaining 46 months data.

The TF model expresses the daily mean streamflow as:

$$\boldsymbol{Y_t} - \delta_1 \boldsymbol{Y_{t-1}} - \cdots - \delta_r \boldsymbol{Y_{t-r}} = \varpi_0 \boldsymbol{X_{t-b}} + \varpi_1 \boldsymbol{X_{t-b-1}} + \cdots + \varpi_s \boldsymbol{X_{t-b-s}} \tag{3.1}$$

where $\boldsymbol{Y_t}$ denotes the mean streamflow at day *t* in m^3/min, $\boldsymbol{X_t}$ is the rainfall depth at day *t* in mm/day, *b* is the time delay between rainfall and streamflow in day, *r* and *s* are the orders of time series, and $\delta_1 \cdots \delta_r$ and $\varpi_1 \cdots \varpi_s$ are parameters to be estimated. Using backshift operator and adding a noise term into Eq. (3.1):

$$\boldsymbol{Y_t} = \frac{\omega(\boldsymbol{B})}{\delta(\boldsymbol{B})} \boldsymbol{X_{t-b}} + \boldsymbol{N_t} \tag{3.2}$$

where $\boldsymbol{B}$ is a backshift operator that transforms any time series data such that $\boldsymbol{B}(\boldsymbol{Y_t}) = \boldsymbol{Y_{t-1}}$, $\omega(\boldsymbol{B})$ and $\delta(\boldsymbol{B})$ are backshift polynomials, and $\boldsymbol{N_t}$ is an unexplained noise at time *t*. $\boldsymbol{N_t}$ is to be white-noised by fitting an autoregressive and moving average (ARMA) model, $N_t = \left(\theta(B)/\phi(B)\right) e_t$, where $\boldsymbol{e_t} \sim \boldsymbol{N}(0, \sigma^2)$ and $\phi(\boldsymbol{B})$ and $\theta(\boldsymbol{B})$ are polynomials for error terms, estimated by the Box-Jenkins procedure (Box and Jenkins, 1976). For this study, we assumed there is no delay, i.e., *b* is equal to 0, based on the fact that a daily time interval is too coarse to detect the time delay between the rainfall and

the streamflow in the relatively small study watersheds. The ratio of polynomials, $\omega(\boldsymbol{B})/\delta(\boldsymbol{B})$, is called the transfer function and describes how the impact of one unit of rainfall is transferred to streamflow over time (O'Connell and Clarke, 1981; Young, 2003). For simplicity, we set *r* and *s* to 1 and 0, respectively, i.e., daily streamflow after the rainfall decreases by the first order. Rewriting Eq. (3.2) with these restrictions yields:

$$\boldsymbol{Y}_t = \frac{\omega_0}{(1-\delta_1 \boldsymbol{B})} \boldsymbol{X}_t + \boldsymbol{N}_t \tag{3.3}$$

Since streamflow eventually goes to baseflow, $\boldsymbol{Y}_t$ series is stationary and δ_1 is always less than 1. Therefore, Eq. (3.3) can be rewritten as:

$$\boldsymbol{Y}_t = \omega_0 \sum_{i=0}^{\infty} \delta_1^{\,i} \boldsymbol{X}_{t-i} + \boldsymbol{N}_t \tag{3.4}$$

The impacts of unit rainfall on day *t* on streamflow on day *t*, *t+1*, *t+2*, … were calculated by updating Eq. (3.4) by *i* time intervals and taking partial derivatives with respect to $\boldsymbol{X}_t$:

$$
\begin{aligned}
&\partial Y_t / \partial X_t = \omega_0 \\
&\partial Y_{t+1} / \partial X_t = \omega_0 \delta_1 \\
&\partial Y_{t+2} / \partial X_t = \omega_0 \delta_1^2 \\
&\qquad \vdots \\
&\partial Y_{t+i} / \partial X_t = \omega_0 \delta_1^i \\
&\qquad \vdots
\end{aligned}
\tag{3.5}
$$

Eq. (3.5) tells us that δ_1 is a recession constant representing the impacts of unit rainfall decay at a rate of δ_1. As δ_1 is closer to 0, the stream dries up more quickly. $\omega_0, \omega_0\delta_1, \omega_0\delta_1^2, \cdots, \omega_0\delta_1^i, \cdots$ are called the discrete impulse response functions (IRFs). Because each term in IRF indicates the impact of unit rainfall, graphical representation of IRF is equivalent to unit hydrograph (O'connell and Clarke, 1981; Young, 2003). Eq. (3.5) also indicates that the impact of unit rainfall on streamflow on the same day of storm, or peakflow, is solely represented by ω_0. If we convert the units of daily rainfall and streamflow to the total volume of rainfall falling onto a watershed (by multiplying the area of a watershed to rainfall depth) and total volume of streamflow flowing out during the storm day (by multiplying a conversion factor from minutes to day), respectively, ω_0 becomes a dimensionless parameter that indicates the volumetric ratio of streamflow to rainfall. Assuming that, in an intermittent stream, surface runoff contributes to most of the streamflow during the storm day, the dimensionless ω_0 can approximately interpreted as runoff coefficient, or zero-day runoff coefficient, of the watershed. The TF model has an advantage over other hydrologic methods in that this model can take into account antecedent rainfalls. The volume of stormwater runoff is not

only determined by today's rainfall but also by soil moisture and groundwater level affected by antecedent rainfalls. Therefore, runoff coefficient might be overestimated if it is measured after a heavy rainfall event a few days ago. TF models were estimated using the ARIMA procedure in SAS 9.1 (SAS Institute Inc., 2004).

Results

Impervious surface classification

For both Landsat TM images taken in 1991 and 2008, SVM correctly classified 79.3% (46 of 58) of the validation pixels. As intended, impervious and non-impervious surfaces were classified without bias, i.e., 79.3% (23 of 29) pixels were correctly classified for both classes. The weights of slack variables were 35 and 10 for 1989 and 2008 images, respectively. Fig. 3.4 illustrates the impervious surface maps for the two study periods. Overall, impervious surface increased by 5.6% (from 10.9% to 16.5%) in all the study watersheds between the two study periods. On the 1991 map, impervious surface was found mostly in the Shoal Creek watershed located near downtown Austin, but it had expanded to neighboring watersheds in 2008. On both maps, impervious surfaces were the largest in the Shoal Creek watershed. Impervious surfaces covered 68.2% and 74.1% of the watershed area in 1991 and 2008, respectively (Table 3.2). The greatest change occurred in the Walnut Creek watershed. Impervious surface increased by 18.0% (from 39.4% to 57.4%) for this watershed. Of the watersheds in the Hill Country, the Williamson Creek watershed has experienced the largest increase in impervious surface. In this watershed, 13.4% of the watershed area (from 18.0% to 31.4%) changed to

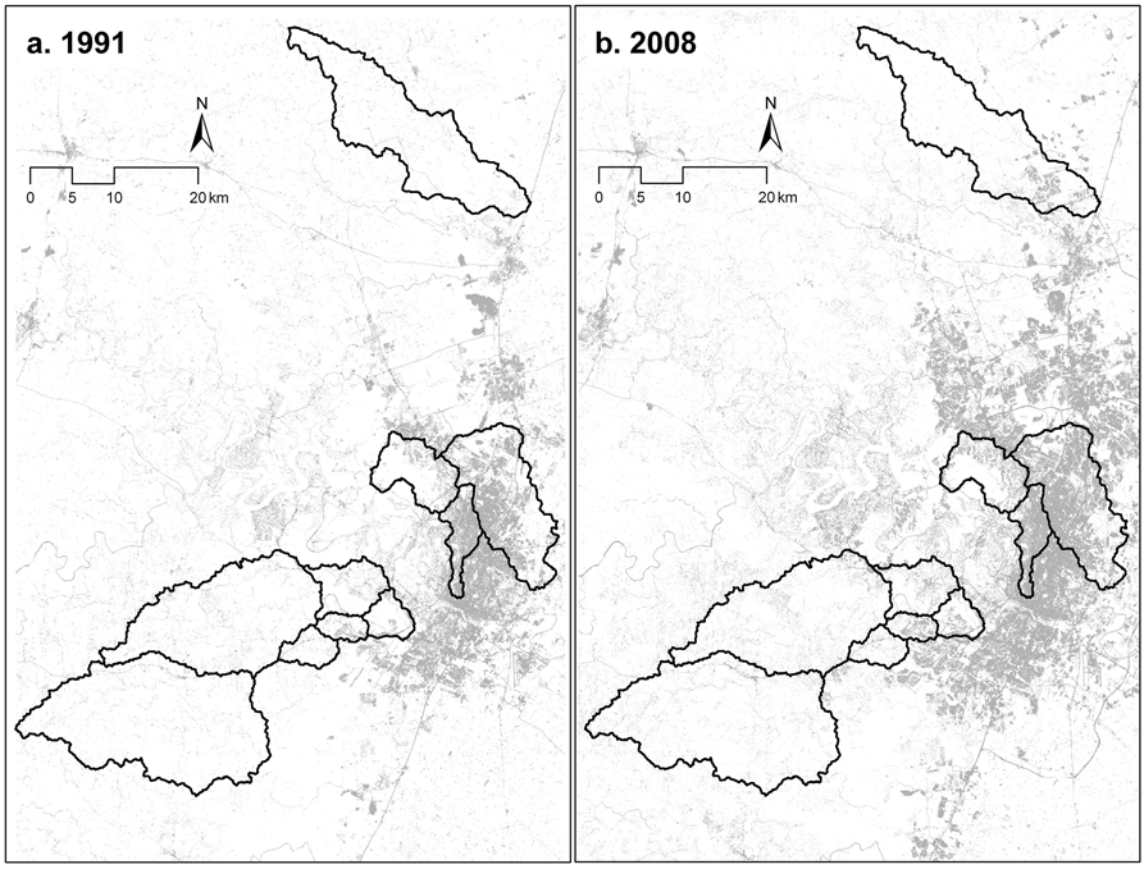

Fig 3.4. Impervious surface classified from Landsat TM images on a) February 8, 1991 and b) February 7, 2008. Grey area represents impervious surfaces.

impervious surface. The watershed with the least impervious surface percentage was the Onion Creek watershed. Less than 5% of the watershed was covered by impervious surface both on 1991 and 2008 maps.

Table 3.2. Impervious surface percentages and two parameters of transfer function (TF) models.

Site*	1991 % impervious surface	2008 % impervious surface	Change in % impervious surface	1989-1992WY $\hat{\omega}_0$	2005-2008WY $\hat{\omega}_0$	1989-1992WY dimension-less $\hat{\omega}_0$ **	2005-2008WY dimension-less $\hat{\omega}_0$ **	2005-2008WY $\hat{\delta}_1$	2005-2008WY $\hat{\delta}_1$	1989-1992WY (AR, MA)$^+$	2005-2008WY (AR, MA)$^+$	% change in $\hat{\omega}_0$	% change in $\hat{\delta}_1$
Walnut (BP)	39.4	57.4	18.0	19.51	21.67	0.20	0.23	0.29	0.29	(1,0)	(0,0)	11.1	-40.0
Shoal (BP)	68.2	74.1	5.9	5.22	6.09	0.23	0.27	0.16	0.16	(0,0)	(1,0)	16.6	-44.7
Berry (BP)	2.1	6.3	4.2	9.62	12.39	0.06	0.08	0.55	0.55	(1,2)	(1,1)	28.7	-13.8
Bull (HC)	18.1	27.6	9.5	4.43	3.35	0.11	0.08	0.59	0.59	(1,3)	(1,1)	-24.4	-12.7
Williamson (HC)	18.0	31.4	13.4	2.56	1.17	0.23	0.10	0.41	0.41	(1,1)	(1,1)	-54.4	-20.1
Slaughter (HC)	6.4	10.4	4.0	1.71	1.54	0.11	0.10	0.41	0.41	(1,4)	(1,4)	-11.1	-43.8
BartonUP (HC)	3.7	6.5	2.8	12.40	11.53	0.08	0.07	0.58	0.58	(1,3)	(1,1)	-7.0	-25.4
BartonMID (HC)	4.7	8.3	3.6	14.43	11.09	0.07	0.06	0.62	0.62	(1,3)	(1,1)	-23.2	-22.3
BartonDOWN (HC)	5.4	9.6	4.2	20.53	12.00	0.10	0.06	0.65	0.65	(1,3)	(1,1)	-41.5	-18.2
Onion (HC)	2.3	3.9	1.6	11.75	11.58	0.05	0.05	0.57	0.57	(1,3)	(1,0)	-1.4	-29.8

* (BP): Blackland Prairie; (HC): Hill Country

** dimensionless $\hat{\omega}_0$ = $\hat{\omega}_0$ [(m^3/min)/(mm/day)] × 1440 (min/day) × 1000 (mm/m) / area of watershed (km^2) × (10^{-6} km^2/m^2)

\+ AR refers the orders of polynomial $\phi(\boldsymbol{B})$ and MA refers to the order of polynomial $\theta(\boldsymbol{B})$ that whitens the unexplained error by rainfall.

Hydrologic change

Three streams in the Blackland Prairie became flashier and more responsive per unit rainfall between the two study periods. TF models indicate that peakflow on the day of a storm rose up higher, while decayed more rapidly after the storm in 2005-2008WY than in 1989-1992WY. For the three streams, $\hat{\omega}_0$s increased by 18.8%, while $\hat{\delta}_1$s decreased by 32.8% on average (Table 3.2).

Unlike the streams in the Blackland Prairie, the streams in the Hill Country became less responsive. For all seven streams, $\hat{\omega}_0$s were lower in 2005-2008WY than in 1989-1992WY. On average, $\hat{\omega}_0$s decreased by 23.3 % between the two study periods (Table 3.2). The stream with the largest change in $\hat{\omega}_0$ was Williamson Creek whose watershed also experienced the largest change in impervious surface percentage among seven watersheds in the Hill Country. For this creek, $\hat{\omega}_0$ decreased by 54.4% and impervious surface increased by 13.4%. For two creeks with the least changes in $\hat{\omega}_0$s (Onion Creek and BartonUP Creek), impervious surfaces also changed the least. To investigate the effects of urbanization on stream hydrology in the Hill Country, we plotted percent change in $\hat{\omega}_0$ over the change in impervious surface percentage between the two study periods (Fig. 3.5a). A strong negative relationship ($R^2 = 0.593$, $p = 0.043$) indicates that peakflow during the day of storm decreased as watersheds became more urbanized. $\hat{\delta}_1$s also decreased in all seven streams in the Hill Country (24.6% on average) in that the streams decay rapidly as watershed became more urbanized, but the

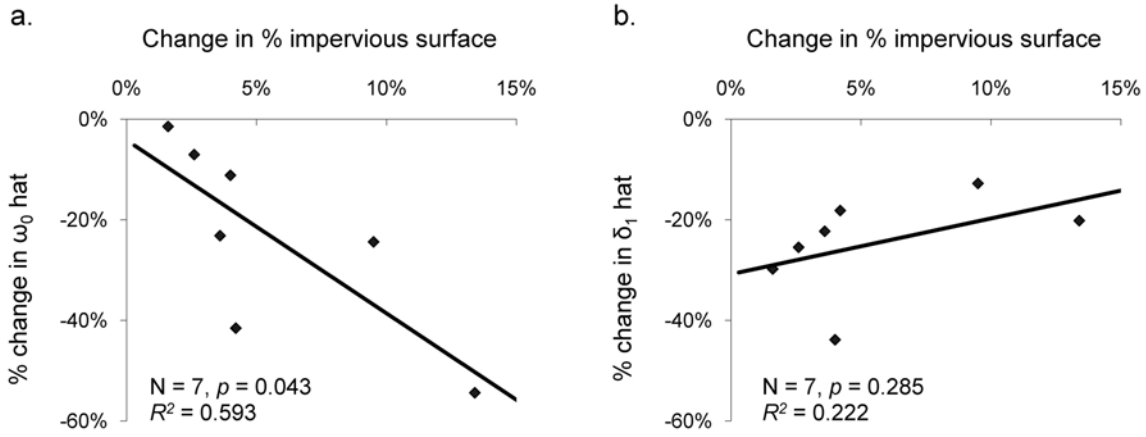

Fig. 3.5. The relationships between the change in impervious surface percentage (in horizontal axis) and a) percent change in ω_0 hat and b) percent changes in δ_1 hat for seven Hill Country sites (in vertical axis).

relationship between percent change in $\hat{\delta}_1$ s and the changes in impervious surface percentage is not statistically significant ($R^2 = 0.222$, $p = 0.285$) (Fig. 3.5b).

IRF plots further illustrate the contrasting patterns in hydrologic changes between the Blackland Prairie and the Hill Country regions. Fig. 3.6 plotted the estimated IRFs for the first 15 days after a storm. For the streams in the Blackland Prairie, the impacts of unit rainfall were initially higher in 2005-2008WY than in 1989-1992WY, but the higher impacts lasted only for one or two days after the storm and remained smaller for the rest of the days (Fig 3.6a to 3.6c). However, the impacts of unit rainfall on the streams in the Hill Country were always lower for 2005-2008WY,

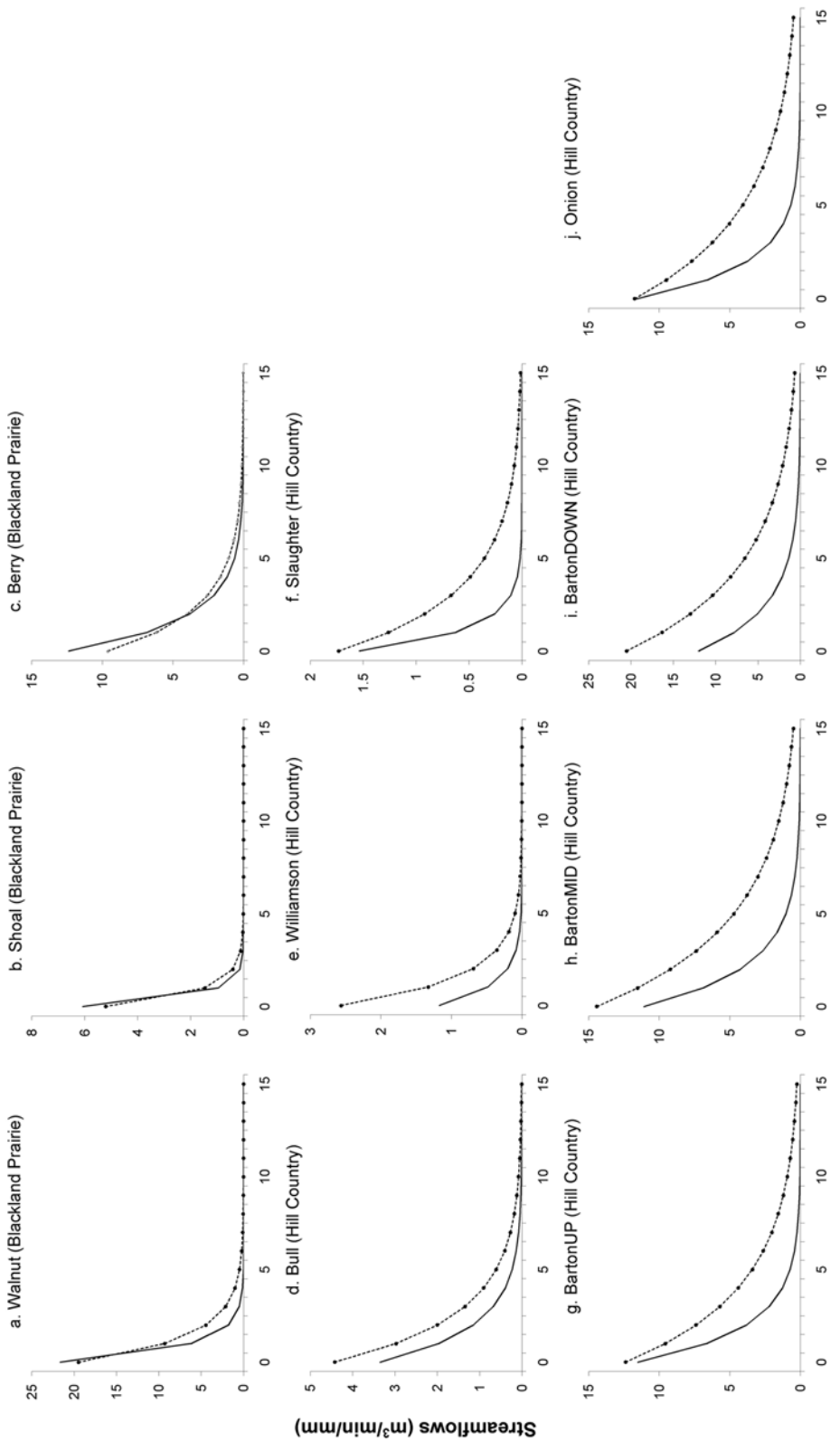

Fig. 3.6. Impulse response functions (IRFs) for the two study periods (the dotted lines with markers for 1989-1992 water year and the solid lines for 2005-2008 water year). Horizontal axis represents the days after a storm and vertical axis represents the impact of one unit of rainfall on streamflow.

suggesting that urbanization decreased peakflow during a storm day (Fig 3.6d to 3.6j). Again, the change in initial impacts between the two study periods is largest in Williamson Creek (Fig 3.6e), while negligible on Onion Creek (Fig 3.6j) and BartonUP Creek (Fig 3.6g).

Discussion and Conclusion

Urbanization does not always make a stream flashier. Of the study streams, only those in the Blackland Prairie (gentle slope watersheds) became flashier during the last two decades. IRF plots illustrate that, as the gentle slope watershed was urbanized, the stream had a larger $\hat{\omega}_0$, i.e., larger peakflow on the same day of a storm, and a smaller $\hat{\delta}_1$, i.e., more rapid recession of streamflow after the storm. In contrast, the streams in Hill Country (hillslope watersheds) became less flashy in that the stream had smaller $\hat{\omega}_0$ s and $\hat{\delta}_1$ s after urbanization. Therefore, we can conclude that urbanization makes stream hydrology drier rather than flashier in hillslope watersheds with less intensive peakflow and longer dry periods.

The comparison of IRFs between the two study periods showed that the streams became more intermittent during the last decades in all study streams. As previously mentioned, this change can be attributed to the overpumpage of the Edwards Aquifer (Bowles and Arsuffi, 1993; Scanlon et al., 2003), but the overpumpage altered the stream hydrology mainly through lowering the baseflow. The stream dryness can be exemplified by the decreases in $\hat{\delta}_1$ s in all study streams regardless of their degrees of

urbanization. Because these streams were hydrologically connected by the Edwards Aquifer, the effect of the overpumpage was not limited to the watershed where the pumpage occurred but extended to neighboring watersheds. In other words, the overpumpage alone cannot explain the different responses between the Blackland Prairie and the Hill Country streams. In the Blackland Prairie, peakflow increased, which suggests that the increase in impervious surface played an important role in stream hydrology of a gentle slope watershed even though the overpumpage lowered the aquifer level and reduced baseflow. Furthermore, the decreases in the peakflow were more evident on hillslope watersheds that were more urbanized, which is contrary to the conventional urban hydrology models. Then, what made the difference between two types of watersheds? Why did the peakflow decrease in the Hill Country watersheds although they also experienced watershed urbanization over the last decades?

We suspect that land grading for the construction resulted in reduced surface runoff in a hillslope watershed. The grading on hillslope creates a stair-stepped or terraced landscape. Fig 3.1 illustrates typical landscapes after urbanization in a hillslope watershed. As described earlier, the Hill County has a stair-stepped landscape even before urbanization due to weathering of the marly interbeds. Marsh and Marsh (1995) and then Woodruff and Wilding (2008) discussed that a hydrologic process on this naturally occurring stair-stepped topography is much more complex than that on non-stair-stepped hillslope. On the stair-stepped watershed, as shown in Fig 3.7, stormwater falling on a tread infiltrates into the ground and moves as subsurface flow until it meets a riser. Then it seeps out to the sidewall of the riser and cascades down to the next tread

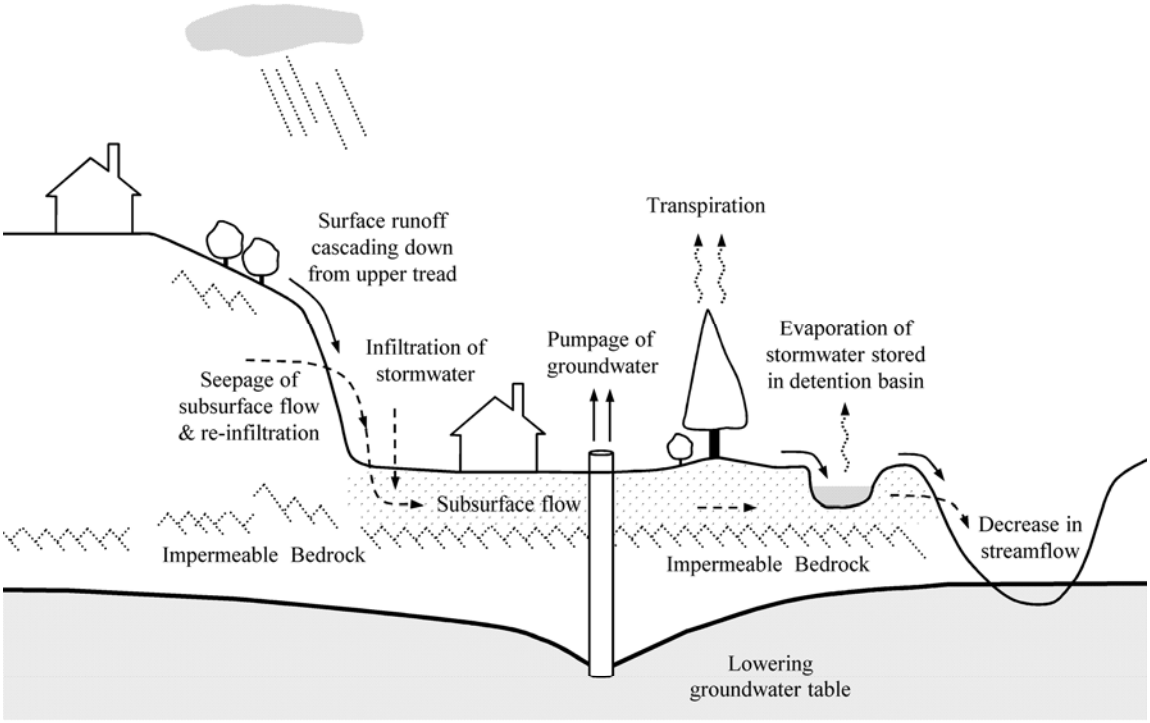

Fig. 3.7. Conceptual model describing stormwater flow over stair-stepped landscape.

below one level. On the tread, stormwater slows down and infiltrates again into the ground. As the infiltration-seepage process continues through a series of risers and treads, the volume and velocity of surface runoff is significantly reduced once it reaches the downstream channel. As a result, stream hydrology is less flashy in the stair-stepped watershed than in other hillslope watersheds with non-stair-stepped hillslope. This process was developed to describe the hydrologic process on a naturally occurring stair-

stepped hillslope, but it can also explain the stream dryness of the study area because land grading likely magnified the steppedness of the hillslope watersheds. Wider and flatter steps created through land grading further decreased the surface runoff in the Hill Country watersheds. In addition to land grading, urbanization also provides an additional stormwater storage area in the form of retention basins nowadays mandated by many municipalities. Water retained in these basins is lost via evapotranspiration if the basin lies over shallow impermeable bedrock that does not permit the infiltration. In the study area, the decrease in surface runoff further dried up downstream because the Edwards Aquifer is mostly recharged through the streambed. Less streamflow during a storm event reduced the aquifer recharge, lowered the aquifer level, and consequently resulted in a longer intermittent period. Fig 3.7 illustrates the hydrologic processes on the stair-stepped landscape altered by urbanization in a hillslope watershed.

It is worth noting other factors that may lead to hydrologic changes in the study watersheds. In this study, we compared stream hydrology of the same watersheds between two study periods. The longitudinal comparison allowed us to control for most natural hydrogeologic characteristics, such as soil and climate because they remained unchanged within this short period of time. Urbanization was the only change having occurred between the two study periods. Therefore, we can attribute the change in hydrologic regimes to urbanization. However, this comparison cannot rule out other potential impacts, such as different development schemes across the study watersheds. Austin divides its territory into five water protection zones and regulated them with varying levels of impervious surface limit, riparian buffer width, and the standards of

sedimentation/infiltration basins (City of Austin, 2008). We originally planned to compare stream hydrology of the different protection zones, but we recognized that the effect of zoning regulation was minor and outweighed by other factors, i.e., slopes of watershed and land grading. Although this study cannot decompose these confounding factors, it would be interesting to evaluate the effect of the watershed regulations on urban hydrology.

Another limitation is related to the method used to estimate watershed permeability. Recently, stormwater management experts suggest to use effective impervious surface area (EIA), impervious surface area only directly connected to drainage system (Lee and Heaney, 2003; Roy and Shuster, 2009). EIA provides more accurate information on watershed permeability, but it has not been widely applied to hydrologic studies because it needs intensive field work to verify what impervious surface area is directly connected to the drainage system. Considering a relatively large study area and the requirement of longitudinal data that cannot be acquired by field survey, we had to use total impervious surface area (TIA) to estimate watershed permeability. Although the analysis based on EIA would be more accurate, we believe that the general conclusion will be the same because in most cases TIA and EIA are strongly positively related.

Current stormwater management schemes are based on maintaining the watershed permeability. For instance, low impact development (LID), a site development technique to maintain predevelopment hydrology, is based on stormwater best management practices (BMPs) that treat stormwater on site (U.S. Environmental

Protection Agency, 2000; Hood et al., 2007; Dietz and Clausen, 2008). Although these management schemes have showed some promising outcomes in gentle slope watersheds, our findings suggest that they may not properly reflect complex hydrogeologic processes in hillslope watersheds. Detention and retention basins may not help preventing the stream dryness in hillslope watersheds because they are likely to decrease the volume of stormwater that reaches the stream channel. Other strategies, such as a site layout plan that adapts to local topography, should be considered. Hillslope watershed attracts more and more residents due to its scenic view. We recommend that watershed management schemes be revised to reflect the local hydrogeological conditions in the hillslope watersheds.

CHAPTER IV

INVESTIGATING ALIEN PLANT INVASION IN URBAN RIPARIAN FORESTS IN A HOT AND SEMI-ARID REGION

Chapter Summary

In this paper, we examined twelve riparian forests along urban-rural gradients in Austin, Texas on 1) the invasion of alien woody species in urban and rural riparian forests, and 2) the relationships among ecosystem invasibility, watershed urbanization, and stream hydrology. Ecosystem invasibility was assessed by relative alien cover (RAC) of the study sites. Stream hydrology was quantified using the transfer function (TF) model. Four years of daily rainfall and streamflow data were used to estimate two parameters of TF models: ϖ_0 (the peak discharge during storm events) and δ_1 (the flow recession after the storms), each of which represents a different attribute of hydrologic regimes. We also measured various environmental variables (15 in total) that characterized the study sites, including impervious surface percentage, area of watershed, two species diversity indices, canopy gap percentage, and several soil nutrient contents. The results indicate that impervious surface percentage was related to δ_1. The more the impervious surface in a watershed, the faster streamflow recedes after the storm, and the longer dry period the riparian forest experienced (R^2=0.722). Impervious surface percentage was also related to RAC (R^2=0.498). Nonmetric multidimensional scaling (NMDS) grouped the environmental variables into five dimensions. One of the dimensions was strongly related to three variables that are known to be associated with hydrologic disturbance:

impervious surface percentage, recession parameter, and canopy gap percentage. Multiple regression analysis of RAC on the five NMDS dimensions shows that the dimension representing hydrologic disturbance significantly affected RAC. This result indicates that watershed urbanization facilitates the invasion of alien species in riparian forests through increasing the level of hydrologic disturbance, particularly drought in a hot and semi-arid region.

Introduction

Riparian forests are prone to the invasion of alien species (Stohlgren et al., 1998; Tickner et al., 2001; Zedler and Kercher, 2004). Floods disturb the riparian forests mechanically as well as by periodically creating an anaerobic environment (Hood and Naiman, 2000; Pettit and Froend, 2001). Once floods recede, the disturbed forests are more easily invaded by alien species that grow faster and are more tolerant to disturbance than native species (Nilsson et al., 1997; Morris et al., 2002; Glenn and Nagler, 2005; Stromberg et al., 2007). Stream channels also help dispersal of the alien species by transporting their propagules from upstream habitats (Moggridge et al., 2009). The invasion of the alien species could threaten biodiversity in a hot and semi-arid region because the riparian forests serve as refugees for regionally rare wetland species (Aguiar and Ferreira, 2005).

Urbanization worsens the invasibility of alien species. Increased impervious surface generates more stormwater runoff, and intensifies the frequency and magnitude of floods in downstreams (Leopold, 1968). Impervious surface also lowers stream

baseflow by decreasing stormwater infiltration into groundwater (Groffman et al., 2002; 2003). Therefore, riparian forests in urban areas suffer from more floods during storm events and droughts during dry periods, and become more vulnerable to invasion by disturbance-tolerant alien species that may be better able to cope with the fluctuating water levels (Medina, 1990; Moffatt et al., 2004; Maskell et al., 2006).

Previous studies attributed the higher invasibility of urban riparian forests to various aspects of urbanization. For instance, King and Buckney (2000) investigated stream and riparian ecosystems in northern Sydney, Australia and found that an increase in soil nutrient level was related to the alien invasion. They discussed that nutrients washed off from fertilized backyards and lawns by stormwater runoff facilitated the invasion of alien species that grow faster than native species in an excessive nutrient environment. In a study of riparian forests in Birmingham, United Kingdom, Maskell et al. (2006) ascribed the abundance of alien species in urban sites to the stream channelization that intensifies flood magnitude. Some studies explained the higher invasibility of urban riparian forests by land use/land cover in surrounding areas. Moffatt et al. (2004) and Burton and Samuelson (2008) reported that alien species in riparian forests increased with urbanization in surrounding landscapes. These studies argued that loss and fragmentation of habitats decreases the ecosystem resistance to the biological invasion. Although the previous studies identified various environmental factors associated with the biological invasion, they recognized hydrologic disturbance as an underlying cause that governed those factors. However, only few have directly related hydrologic disturbance to the invasion of the alien species in urban riparian forests (e.g.,

Greer and Stow, 2003; Burton et al., 2009). This may be due to the difficulty in quantifying hydrologic disturbance.

The objective of this study is to examine whether urbanization facilitates alien species invasion by raising the level of hydrologic disturbance. To quantify hydrologic disturbance, we used a transfer function (TF) model that characterizes the dynamic relationship between rainfall and streamflow. TF models were estimated from four-year daily rainfall and streamflow data of twelve streams along urban-rural gradients in Austin, Texas. We also measured various environmental variables potentially affecting the invasibility of riparian forests. Based on the relationships between the environmental variables and ecosystem invasibility assessed by surveying woody vegetation communities near the stream gaging stations, we investigated factors that lead to the biological invasion in urban riparian forests.

Materials and Methods

Study sites

The study area is Austin, Texas, one of the fast growing cities in the United States. Population increased from 465,622 in 1990 to 757,688 in 2008 (U.S. Census Bureau, 2009) and correspondingly many natural habitats have been converted to urban areas. The study area shown in Fig. 4.1 is located where two major ecoregions meet. The eastern half of the study area is the Blackland Prairie ecoregion, a flat to rolling plain with deeply incised streams. This ecoregion has deep and organic rich clay soil (Soil Conservation Service, 1974). Across the Balcones Escarpment to the west is the Hill

Country, an eastern end of the Edwards Plateau ecoregion. This region has a rugged landscape with numerous hills and valleys formed by exposed limestone bedrocks (Marsh and Marsh, 1995; Woodruff Jr. and Wilding, 2008). The soil in this region is shallow and composed of gravel and clay loam weathered from the underlain Cretaceous limestone bedrock (Soil Conservation Service, 1974). The study area is underlain by the Edwards Aquifer, a shallow karst aquifer vulnerable to surface water contamination (Bowles and Arsuffi, 1993). Many artesian springs fed by the Edwards Aquifer are also found in this area. Except human land uses, the study area is covered by mixed forests dominated by live oak (*Quercus virginiana*), Ashe's juniper (*Juniperus ashei*), and honey mesquite (*Prosopis glandulosa*) (McMahan et al., 1984). The climate is subtropical with hot summer and mild winter. Mean annual precipitation is 810mm mostly falling in spring and fall [National Climatic Data Center (NCDC), 2009]. Snow is rare.

We studied twelve remnant riparian forests in Austin (Fig. 4.1). The study sites were selected to couple the vegetation survey data with the daily mean streamflow data collected by the U.S. Geological Survey (USGS). All streams are intermittent. Because Barton Creek and Onion Creek are monitored by multiple stations, the total number of streams is seven. Five streams are tributaries of the Colorado River, while Plum Creek and Berry Creek are tributaries of the Guadalupe River and the Brazos River, respectively.

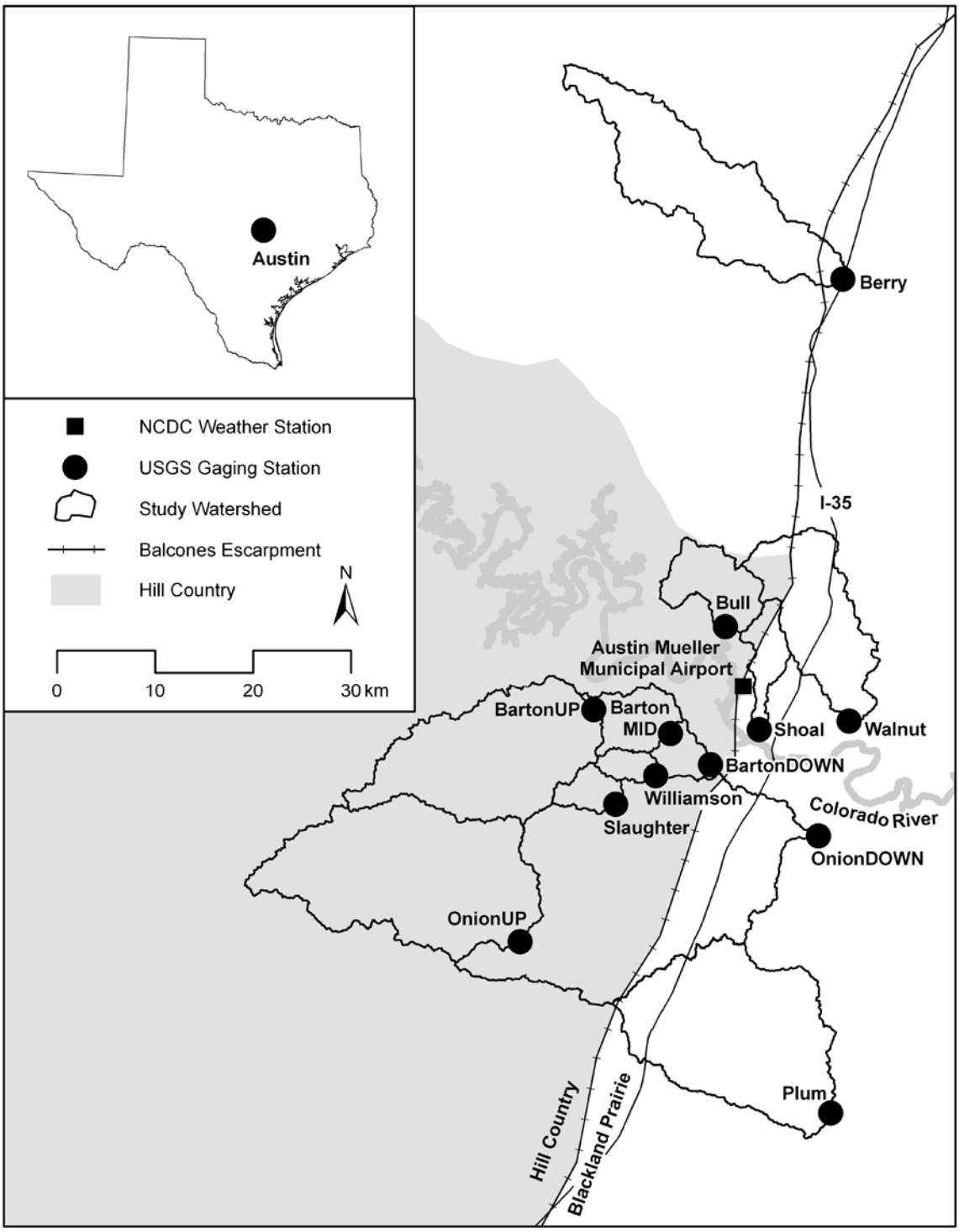

Fig. 4.1. Locations of twelve study sites.

Impervious surface estimation

We estimated the degree of watershed urbanization by measuring impervious surface percentage. This section highlights key procedures. Detailed procedures are described in Chapter II and III. An impervious surface map was generated from Landsat TM image acquired on February 7, 2008. We selected this image because it is cloud free and taken in winter when impervious surface under tree canopy is more easily detectable. The image was classified by support vector machine (SVM) due to its ability to improve classification accuracy particularly for image pixels near the margin between land cover classes (Burges, 1998; Foody and Mathur, 2006). Training and validation pixels were selected by referring fine resolution aerial photographs taken in 2008. ENVI 4.5 was used for the image classifications (ITT Visual Information Solutions, 2008). Once impervious surface was classified, impervious surface percentage was calculated for a watershed delineated from 1 arc-second USGS National Elevation Dataset using BASINS.

Quantifying hydrologic regime

For each stream, the TF model was estimated using daily rainfall and daily mean streamflow for four water years (WY) between October 2004 and September 2008. The daily rainfall data were observed at Austin Mueller Municipal Airport (NCDC COOP ID: 410428) approximately at the center of the study area. Although there were other weather stations near some of the study stream gaging stations, we did not use the data from those stations because they did not measure the rainfall from midnight to midnight

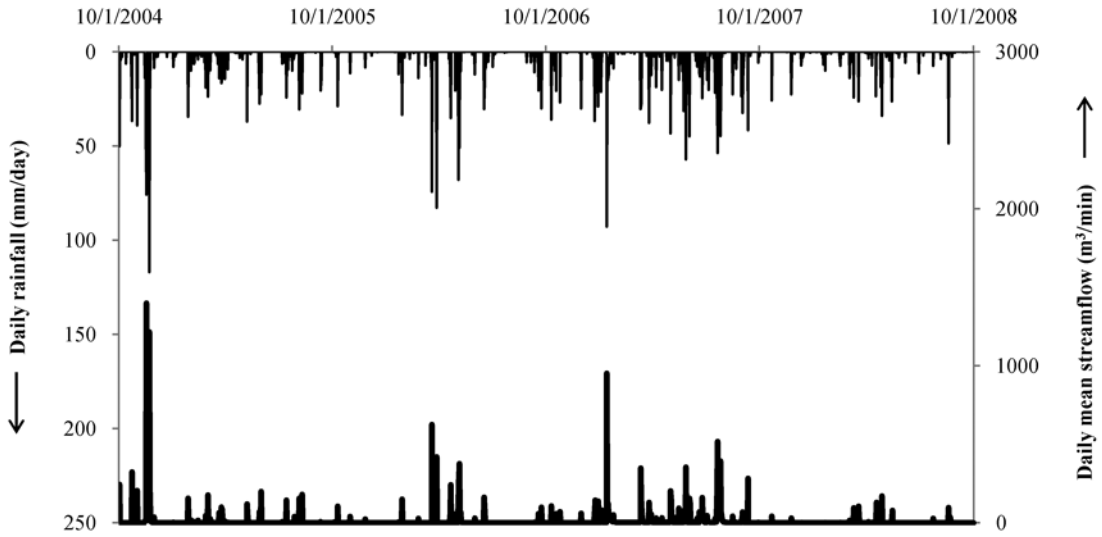

Fig. 4.2. Daily hyetograph and hydrograph for four water year study period. Daily rainfall depth and daily mean streamflow were measured at Austin Mueller Municipal Airport and Shoal Creek gaging station (the most urbanized stream), respectively.

(e.g., the Morgan weather station, the one near Plum Creek, read the rain gage at 8am every day). The mean annual precipitation during the 4WY study period was 863mm, which is higher than the long term average (810mm). Fig. 4.2 illustrates the daily hyetograph and hydrograph for Shoal Creek (the one near downtown Austin).

TF model expresses the daily mean streamflow as:

$$Y_t = \frac{\varpi(B)}{\delta(B)} X_t + N_t, \quad N_t = \frac{\theta(B)}{\phi(B)} e_t \tag{4.1}$$

where, Y_t denotes the mean streamflow at day *t* in m^3/min, X_t is the rainfall depth at day *t* in mm, *B* is the backshift operator, $\varpi(B)$, $\delta(B)$, $\theta(B)$, and $\phi(B)$ are the backshift polynomials estimated by Box and Jenkins' (1976) procedure, N_t is unexplained noise at time *t*, and e_t is true white noise. For simplicity, we restricted the model by setting the orders of polynomial $\varpi(B)$ and $\delta(B)$ by 0 and 1, respectively. The simplified TF models can be written as:

$$Y_t = \frac{\varpi_0}{1 - \delta_1 B} X_t + N_t \tag{4.2}$$

where, ϖ_0 is a parameter of the 0 order term in the polynomial $\varpi(B)$, and δ_1 is a parameter of the first order term in the polynomial $\delta(B)$. Because daily streamflow rises during a storm event and ultimately returns to baseflow, rainfall-streamflow series is stationary and δ_1 must have a value between 0 and 1. Eq. (4.2) can be expressed as an infinite sum of weighted rainfalls on previous days:

$$Y_t = \varpi_0 \sum_{i=0}^{\infty} \delta_1 X_t + N_t \tag{4.3}$$

The parameters of X_t, X_{t-1}, X_{t-2}, …X_{t-i} …, in Eq. (4.3) were given as ϖ_0, $\varpi_0\delta_1$, $\varpi_0{\delta_1}^2$,…, $\varpi_0{\delta_1}^i$, …, and can be interpreted as the impacts of unit rainfall at day *t*

on streamflow at day *t*, *t-1*, *t-2*, …., *t-i*, …. Because $0 < \delta_1 < 1$, the impact of unit rainfall on streamflow is ϖ_0 at day 0, and decays exponentially at the rate of δ_1. Therefore, ϖ_0 represents the impact of unit rainfall on the streamflow on a same day and δ_1 indicates how fast streamflow decays after a storm. Higher ϖ_0 means higher magnitude of streamflow during storm events and higher δ_1 means slower recession of streamflow after the storm. The TF models were estimated by the maximum likelihood method using the ARIMA procedure in SAS 9.1 (SAS Institute Inc., 2004).

Previous studies showed that the TF model is equivalent to other conventional hydrologic methods. For instance, graphical representation of the daily impacts is equivalent to unit hydrograph, commonly used in hydrologic analysis (O'connell and Clarke, 1981; Young, 2003). Also, we can estimate zero-day runoff coefficient from the TF model by simply converting the unit of ϖ_0 so that ϖ_0 represents the ratio of the total volume of streamflow flowing out during a storm day to the total volume of rainfall falling onto a watershed. Although the TF model is conceptually equivalent to the existing methods, it has an advantage on incorporating antecedent rainfalls in parameter estimation. A watershed-stream system has a strong memory on rainfalls on previous days, i.e., it stores stormwater in various forms, such as reservoir, soil moisture and groundwater. Ignoring the antecedent rainfalls significantly lowers the prediction accuracy of streamflow. Many studies showed that TF models successfully predicted streamflow using rainfall data in various time intervals (e.g., Young and Beven, 1994; Nwakalila, 2001; Young, 2003; Farahmand et al., 2007).

Vegetation sampling

We surveyed woody vegetation communities near USGS gaging stations during October 2008 using a line intercept method (Caratti, 2006). We placed two 30m line transects parallel to stream bank – the first transect along the stream bank and the second one 5m apart from the stream bank. Transects followed the curvature of the streamline. Lengths of canopies intersecting the transect lines for all woody vegetation taller than 0.6m were measured. To exclude the effect of gaging stations, such as physical damage during installation and regular maintenance, the transects began at 10m downstream from the station. In the case that the transects passed over areas that were not accessible (e.g., fenced private lands) or significantly disturbed by human activities (e.g., street trees and lawns), we selected an alternative location in the following order: 1) across the stream from the gaging station, 2) toward the upstream direction at the same side of the station, 3) toward the upstream direction across the stream from the station. Nomenclature and native status of species followed the USDA NRCS PLANTS database (http://plants.usda.gov). Soil samples were taken at a depth of 30cm in the middle of each transect and sent to the Texas A&M University Soil, Water and Forage Testing Laboratory for analysis of pH, nitrate-N (NO_3-N), phosphorus (P), potassium (K), calcium (Ca), magnesium (Mg), sulfur (S), and sodium (Na) concentrations.

Data analysis

We summarized the vegetation survey data to reflect several characteristics of the riparian community. The invasibility of the riparian forest was estimated by relative

alien cover (RAC) (Magee et al., 2008). Canopy gap percentage was calculated to indirectly measure the level of ecosystem disturbance, i.e., the greater the canopy gap, the more severe disturbance the riparian forest experienced. Species richness and Shannon diversity index were also calculated to measure the species diversity of the vegetation communities (Magurran, 1988). Ultimately analyzed variables added up to 15 environmental variables, including watershed characteristics, hydrologic regimes, vegetation community structures, and soil nutrient contents. These variables are listed in Table 4.1.

Preliminary analyses (paired *t*-tests) showed that there was no significant difference between the first and second transects on all variables including RAC, two diversity indices, canopy gap percentage, and soil nutrient contents. Therefore, data of the first and second transects were pooled for the rest of the analyses. Additional tests (*t*-tests) were conducted to compare the potential effects of different environmental or sampling conditions, such as different ecoregions or different sampling locations (i.e., between upstream and downstream of the USGS gaging stations, or between the sites on the same side and across the stream from the USGS stations). Again, no statistically significant differences were found between all aforementioned variables, and thus these variations were not considered in subsequent analyses.

Because many environmental variables confound each other, they need to be decorrelated or reduced to evaluate the net effect on the invasibility of the riparian forest. We extracted the smaller number of dimensions from a 15-dimensional input space using nonmetric multidimensional scaling (NMDS) (Everitt, 2005). The distances

Table 4.1. Description of variables analyzed in this study.

Variables	Description
Invasibility of riparian forest	
Relative alien cover (RAC)	(sum of alien species cover / total species cover) × 100% (Magee et al., 2008)
Watershed characteristics	
Area of watershed	Delineated using national elevation data (NED) by BASINS (km^2)
Impervious surface (%)	Classified from 2008 Landsat TM image by support vector machine (SVM)
Stream hydrology	
$\hat{\varpi}_0$	Scale parameter from TF model (m^3/min/mm)
$\hat{\delta}_1$	Recession parameter from TF model [(m^3/min)/(m^3/min)]
Community structure	
Canopy gap (%)	(Lengths not covered by canopy of any woody species / length of transect) × 100%
Species richness	Total number of woody plant species (Magurran, 1988)
Shannon diversity index	$-\sum_{i=1}^{S} p_i \ln p_i$ where, S = number of species, p_i = the relative abundance of species i (Magurran, 1988)
Soil nutrient contents*	
pH	-
NO_3-N	(ppm)
P	(ppm)
K	(ppm)
Ca	(ppm)
Mg	(ppm)
S	(ppm)
Na	(ppm)

* average concentrations in soil samples taken at two transects

between the pairs of twelve sites in the input space were used to construct a dissimilarity matrix. To level out different measurement units for the environmental variables, they were rescaled from 0 to 1 prior to constructing the dissimilarity matrix. The number of dimensions to be extracted was determined based upon stress values calculated by 1-norm Minkowski distance between original and estimated dissimilarities. The varimax method was used to rotate the dimensions. Once NMDS extracted dimensions, we performed a regression analysis to predict RAC using the NMDS dimensions. Because the sample size is small (n=12) and vulnerable to the violation of the normality assumption, all statistical tests were based upon a bootstrapping procedure. 95% confidence intervals (CIs) were constructed from 999 resampled datasets using the bias correction with acceleration constant (BCa) method. vegan (Oksanen, et al., 2009) and boot (Canty and Ripley, 2009) packages in R were used to conduct NMDS and bootstrapping regression analysis, respectively.

Results

The vegetation survey of the twelve riparian forests documented thirty-four woody species (Table 4.2). Dominant native species included Pecan (*Carya illinoinensis*), Sugarberry (*Celtis laevigata*), Netleaf Hackberry (*Celtis reticulata*), Green Ash (*Fraxinus pennsylvanica*), American Elm (*Ulmus americana*), and Cedar Elm (*Ulmus crassifolia*). These species were found at more than half of the study forests. Of the thirty-four species, four were alien species. Those species include Chinaberry (*Melia azedarach*), Glossy Privet (*Ligustrum lucidum*), Chinese Privet (*Ligustrum sinense*), and

Table 4.2. Woody native and alien species (taller than 0.6m) found at twelve study sites.

Scientific name	Common name	Number of sites observed
Alien species		
Ligustrum lucidum	Glossy Privet	4
Ligustrum sinense	Chinese Privet	1
Melia azedarach	Chinaberrytree	8
Triadica sebifera	Chinese Tallow	3
Native species		
Acer negundo	Boxelder	4
Amorpha fruticosa	Desert False Indigo	1
Carya illinoinensis	Pecan	7
Celtis laevigata	Sugarberry	9
Celtis occidentalis	Common Hackberry	2
Celtis reticulate	Netleaf Hackberry	8
Cephalanthus occidentalis	Common Buttonbush	4
Cornus drummondii	Roughleaf Dogwood	5
Diospyros texana	Texas Persimmon	1
Eysenhardtia Texana	Texas Kidneywood	1
Fraxinus pennsylvanica	Green Ash	7
Fraxinus texensis	Texas Ash	4
Ilex deciduas	Possumhaw	4
Ilex vomitoria	Yaupon	2
Juglans major	Arizona Walnut	1
Juglans nigra	Black Walnut	3
Juniperus ashei	Ashe's Juniper	1
Morus rubra	Red Mulberry	4
Parkinsonia aculeata	Jerusalem thorn	1
Platanus occidentalis	American Sycamore	5
Populus deltoids	Eastern Cottonwood	2
Quercus macrocarpa	Bur Oak	1
Quercus shumardii	Shumard's Oak	1
Rhus copallina	Winged Sumac	2
Robinia Pseudoacacia	Black Locust	2
Salix nigra	Black Willow	3
Sideroxylon lanuginosum	Gum Bully	3
Taxodium distichum	Bald Cypress	1
Ulmus Americana	American Elm	8
Ulmus crassifolia	Cedar Elm	8

Table 4.3. The parameter estimates of transfer function (TF) models and the relative alien cover (RAC) of twelve study sites.

USGS ID	Site Name*	Ecoregion	Area of watershed (km^2)	% impervious surface
08158600	Walnut Creek	Blackland Prairie	138.4	57.4
08156800	Shoal Creek	Blackland Prairie	33.0	74.1
08159000	OnionDOWN Creek	Blackland Prairie**	838.0	13.1
08105100	Berry Creek	Blackland Prairie	213.9	6.3
08172400	Plum Creek	Blackland Prairie	287.0	7.1
08154700	Bull Creek	Hill Country	58.7	27.6
08158920	Williamson Creek	Hill Country	16.3	31.4
08158840	Slaughter Creek	Hill Country	22.7	10.4
08155200	BartonUP Creek	Hill Country	231.8	6.5
08155240	BartonMID Creek	Hill Country	278.0	8.3
08155300	BartonDOWN Creek	Hill Country	301.6	9.6
08158700	OnionUP Creek	Hill Country	320.2	3.9

* The surfixes, "UP", "MID", and "DOWN" represent the relative locations of USGS gaging stations at Barton Creek and Onion Creek
** The watershed lying on two ecoregions

Chinese Tallow (*Triadica sebifera*). Chinaberry (*Melia azedarach*) was the most widespread alien woody species in the study area. Eight of twelve sites were invaded by *M. azedarach*.

Impervious surface covered 18% of the area of the twelve study watersheds altogether. Table 4.3 presents the percent impervious surface of the study watersheds. Shoal Creek watershed located near downtown Austin had the highest impervious surface percentage at 74%. Walnut Creek was the second most urbanized watershed (57%). The watershed with the least impervious surface was OnionUP Creek (4%), the southwesternmost watershed in the study area. Berry Creek (6%) and BartonUP Creek

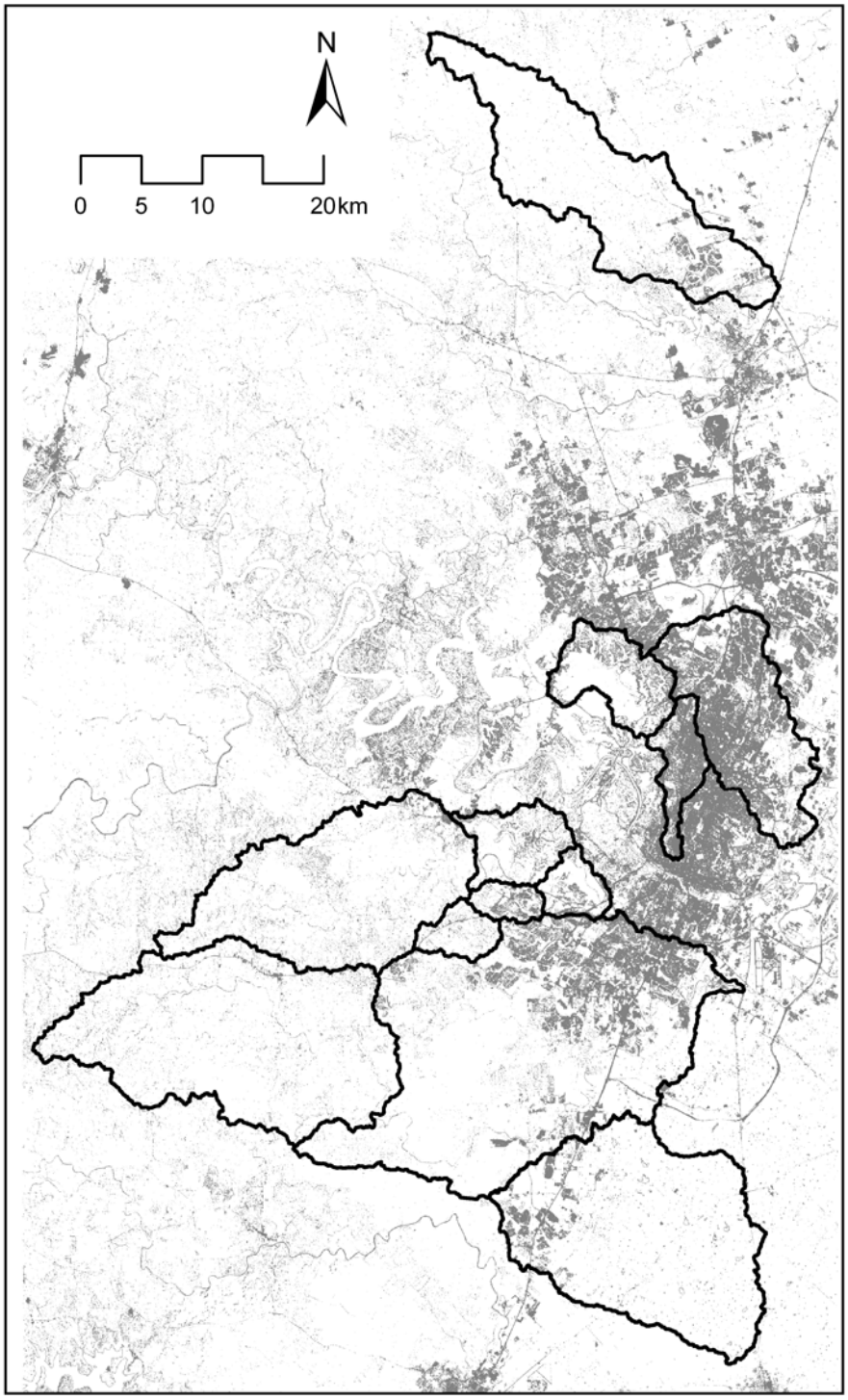

Fig. 4.3. Impervious surface (in halftone) detected from Landsat TM images (February, 2008) by support vector machine.

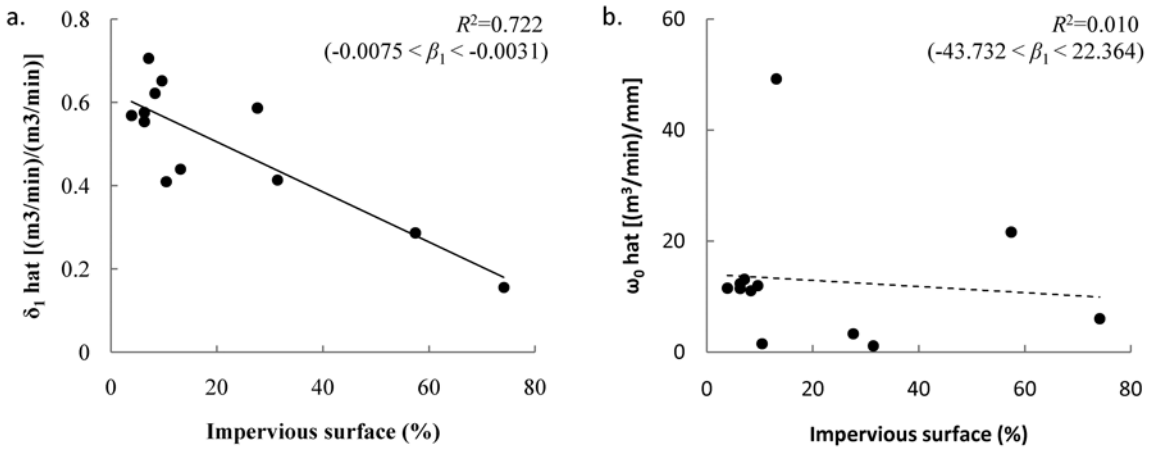

Fig 4.4. Bivariate regressions of two parameter estimates of transfer function (TF) model (ω_0 hat and δ_1 hat) on imperivous surface percentage with 95% bootstrapping confidence interval for regression slope (β_1) in parenthesis. A soild regression line indicates a significant relationship, while a dotted line represents an insignificant relationship at α=0.05.

(7%) also had low impervious surface percentages. Fig. 4.3 illustrates the impervious surface map generated from the Landsat TM image by SVM.

Impervious surface percentage was found to be significantly related to $\hat{\delta}_1$ (Fig. 4.4a). The regression analysis showed the strong negative effect of impervious surface percentage on $\hat{\delta}_1$ (R^2 = 0.722, the regression slope significantly different from 0 at α=0.05), indicating that as a watershed is increasingly urbanized, streamflow more rapidly recedes after a storm. The relationship between impervious surface percentage and $\hat{\omega}_0$ was not statistically significant (Fig. 4.4b).

Table 4.4. Pearson's correlations between four dimensions extracted by nonmetric multidimensional scaling (NMDS) and 15 environmental variables.

Variables	NMDS 1	NMDS2	NMDS3	NMDS4	NMDS5
Area of watershed	-0.429	-0.813*	0.174	0.275	0.038
% Impervious surface	0.332	0.049	-0.832*	-0.415	0.095
$\widehat{\varpi}_0$	-0.389	-0.857*	-0.152	0.113	-0.127
$\hat{\delta}_1$	-0.245	-0.015	0.925*	0.018	0.088
% canopy gap	0.207	0.219	-0.583*	0.323	0.050
Species richness	0.638*	-0.344	0.516	-0.394	0.089
Shannon diversity Index	0.597*	-0.514	0.338	-0.391	-0.144
pH	0.745*	0.424	0.236	0.384	0.100
NO_3-N	-0.385	-0.677*	-0.180	0.179	0.021
P	-0.678*	-0.088	-0.074	-0.254	0.328
K	-0.850*	0.202	-0.050	-0.231	0.254
Ca	0.829*	-0.456	-0.093	0.101	-0.112
Mg	-0.033	0.249	0.741*	0.042	0.081
S	0.041	0.176	0.214	-0.187	-0.673*
Na	-0.716*	0.242	0.242	-0.425	0.018

* significant at α=0.05

NMDS extracted five dimensions from the 15 environmental variables (Table 4.4). The five-dimensional model was selected because stress values, an indicator of the overall error not captured by reduced dimensions, i.e., began to stabilize from this model. The first dimension (NMDS 1) indicates species diversity and soil nutrient levels of a riparian ecosystem: it was significantly related to species richness, Shannon diversity index, soil pH, P, K, Ca, and Na. The second dimension (NMDS 2) generally represented flow magnitude: it was found to be significantly related to the area of watershed, $\widehat{\varpi}_0$, and soil N. The third dimension (NMDS 3) can be considered as an

Table 4.5. 95% bootstrapping confidence intervals (CIs) of regression slopes of relative alien cover (RAC) on five dimensions extracted from nonmetric multidimensional scaling (NMDS) (R^2 = 0.764).

		95% CIs	
NMDS Dimensions	Parameter estimates	Lower Bound (2.5%)	Upper Bound (97.5%)
Intercept	0.134	-	-
NMDS1	0.065	-0.383	0.209
NMDS2	0.027	-0.132	0.446
NMDS3*	-0.221	-0.735	-0.004
NMDS4	-0.020	-0.197	1.631
NMDS5	0.315	-0.074	0.708

* the regression slope statistically significant different from 0 at α =0.05

indicator of hydrologic disturbance. This dimension was significantly related to $\hat{\delta}_1$, impervious surface percentage, and canopy gap percentage (r = -0.583). Two other dimensions did not reflect any distinct environmental characteristics.

We investigated the effects of various environmental factors on the ecosystem invasibility by regressing RAC on the five NMDS dimensions. The result showed that only the third dimension (NMDS 3) significantly affected RAC of the riparian forest controlling the effects of other environmental variables (the regression slope significantly different from 0 at α=0.05) (Table 4.5). Because this dimension represents the degree of hydrologic disturbance, we can conclude that hydrologic disturbance contributed to the increased invasibility of the urban riparian forests. Bivariate regression analyses between RAC and 15 environmental variables also showed that RAC

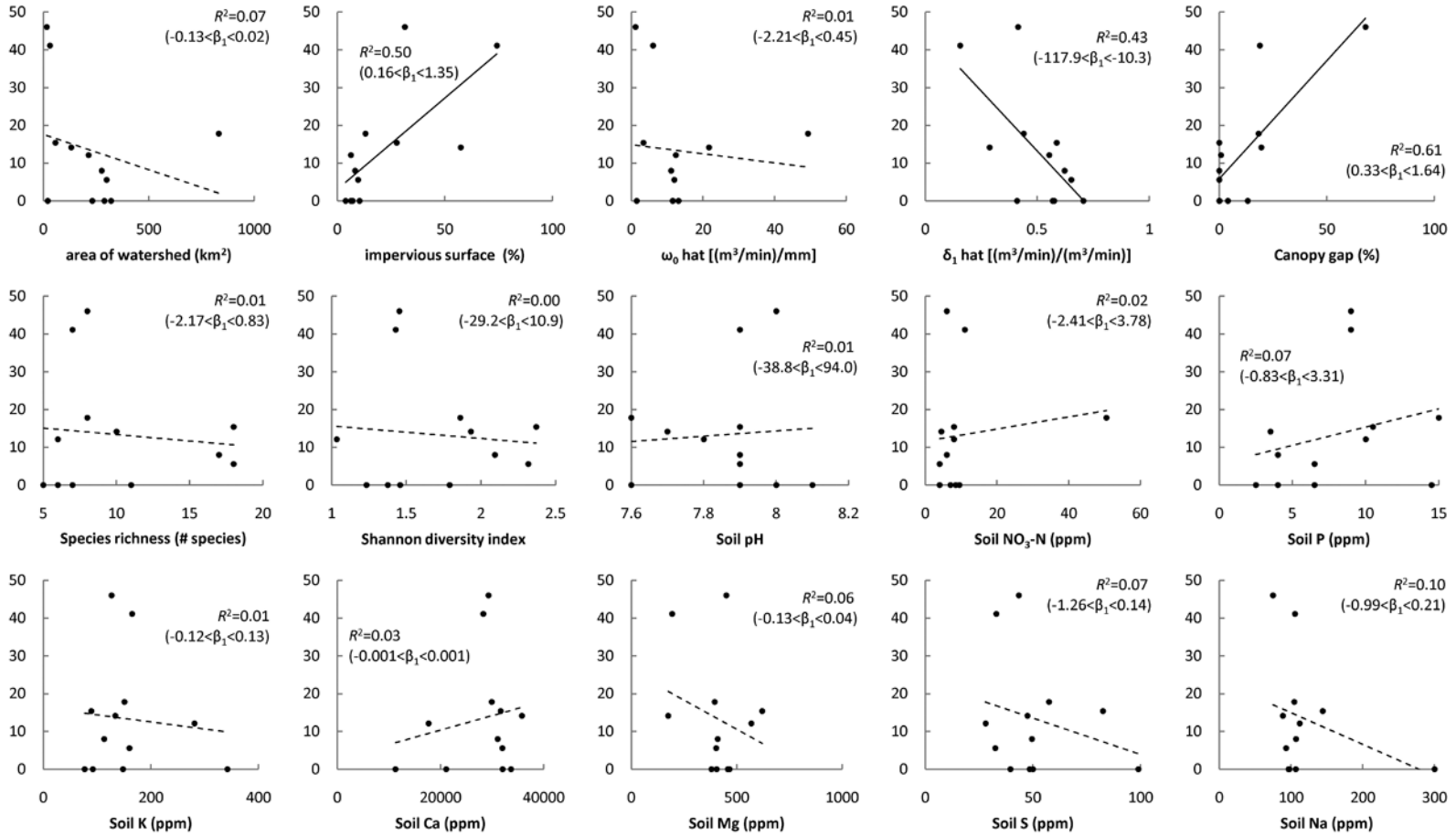

Fig. 4.5. Bivariate regressions of relative alien cover (RAC) on 15 environmental variables with 95% bootstrapping confidence interval for regression slope (β_1) in parenthesis. Y-axis represents RAC in percentage. Solid regression lines indicate significant relationships, while dotted lines represent insignificant relationships at α=-0.05.

was significantly affected by the three variables related to the third NMDS dimensions: $\hat{\delta}_1$, impervious surface percentage, and canopy gap percentage (Fig. 4.5).

Discussion

In this study, we found that RAC was related to three environmental variables: impervious surface percentage of a watershed, recession parameter $\hat{\delta}_1$, and canopy gap percentage. NMDS also showed these three variables covary with each other. As mentioned earlier, canopy gap is an indicator of ecosystem disturbance. The strong positive relationship between impervious surface percentage and canopy gap percentage suggests that urbanization increases the ecosystem disturbance of riparian forests. From these results, we can conjecture a causal pathway from watershed urbanization to alien species invasion: 1) urbanization alters stream hydrology of a watershed by lengthening dry periods; 2) the altered hydrologic regime disturbs riparian forests and provides space for invasion by alien species; 3) alien species replace a native competitor within a same regenerating cohort; and 4) after several generations, the riparian forests become dominated by the alien invaders.

As expected, hydrologic disturbance appears to play a critical role in the invasion of riparian forests in the study area, but the inferred mechanism in this study differs from what conventional urban hydrologic models assert. According to the conventional models, urbanization facilitates biological invasion in a riparian forest by increasing peakflow. However, in the study area, RAC was not significantly related to $\hat{\varpi}_0$, but strongly related to $\hat{\delta}_1$. No significant relationship between RAC and $\hat{\varpi}_0$ is apparently

due to the very large effect of the area of watershed on $\widehat{\varpi}_0$ overwhelming other effects. Thus, for a more accurate analysis of the effect of urbanization on peakflow, we need to control for the effect of the area of watershed, as we did in a previous study (see Chapter III), by longitudinally comparing stream hydrology of the same watershed before and after urbanization. In the previous study, we showed that urbanization did not always increase peakflow in the study area. Peakflow increased only in the Blackland Prairie region during the last two decades when Austin experienced rapid urbanization, but in the Hill Country region, peakflow decreased during the same period. In the same study, we also found that urbanization always decreased $\hat{\delta}_1$, suggesting that urbanization dried up streams in the study area, due to the alteration of hillslope topography and overpumpage of groundwater. Combining these findings with the ones of the present study, we can conclude that, the study area suffered from hydrologic drought with a longer intermittent period as a result of watershed urbanization. Decreased peakflow implies that urbanization facilitated biological invasion in riparian forests not by increasing flood magnitude, but by hydrologic drought caused by lower baseflow.

Hydrologic drought in urban riparian forests has been reported in previous studies. For instance, Moffatt et al. (2004) reported drier and more alkaline soils, and more alien plant species in urban than rural riparian forests in Manitoba, Canada. Groffman et al. (2003) also found that in Baltimore, USA, urban riparian forests experienced more dry conditions, indicated by high soil denitrification potential. Burton et al. (2009) also exhibited that watershed urbanization was related negatively to baseflow in an adjacent stream and positively to flood-intolerant species in Georgia,

USA. Many native riparian species adapt to a mesic environment, and are less likely to survive in a drier condition. Therefore, the droughts shifted riparian vegetation compositions to the ones invaded by drought-tolerant alien species. The Baltimore study showed that urban riparian forests consisted of twice as many upland invaders as rural ones. The drought effect could be much more serious in a hot and semi-arid climate region where evapotranspiration quickly depletes moistures in soil. In this region, water is a limiting factor for the plant growth and groundwater is often the sole source of water for phreatophytic riparian species. Lowering groundwater level by watershed urbanization could make a riparian forest less habitable for the native riparian species (Snyder and Williams, 2000; Horton and Clark, 2001). In our study, canopy gap percentage was significantly related to impervious surface percentage (R^2=0.172) and to $\hat{\delta}_1$ (R^2=0.276). These relationships imply that urbanization-induced drought is so severe that many woody species cannot establish in the study sites. A positive relationship between canopy gap percentage and RAC further shows that canopy gaps created by drought were easily invaded by alien species. Less competition with native counterparts made the urban riparian forests more vulnerable to invasion by disturbance-tolerant alien species. Similar patterns were also found in previous studies that investigated the invasion of *Tamarix spp*., rapidly spreading along riparian forests in U.S. southwest. These studies showed that the abundance of *Tamarix spp*. was related to the altered hydrologic regime, particularly the flood regulation by dams in upstreams that increased the drought stress to riparian forests (Glenn and Nagler, 2005; Stromberg et al, 2007). Again, no strong relationship between $\widehat{\varpi}_0$ and canopy gap percentage (R^2=0.008) implies

that peakflow, an indicator of flood magnitude, was not a dominant type of disturbance of these sites.

Finally, no strong relationships between two species diversity indices (species richness and Shannon diversity index) and RAC in this study results suggest that Elton's theorem, a theorem stating that an ecosystem with higher species diversity is more resistant to biological invasion (Elton 1958), cannot explain the invasibility of urban riparian forests. Lack of an effect of species diversity has been reported in many studies that were conducted in highly disturbed ecosystems. These studies argued that under severe disturbance regimes the effect of disturbance outweighs the effect of diversity and allogenic process governs ecological succession (Planty-Tabacchi et al., 1995; Stohlgren et al., 1999; von Holle, 2005; Maskell et al., 2006, but see Levine, 2000). In other words, biological invasion was primarily determined by the disturbance regime, but not by interspecific competition between native and alien species in our study sites.

Conclusion

In this study, we investigated twelve riparian forests in Austin, Texas and found that watershed urbanization increased the invasibility of urban riparian forests. We infer that the change in hydrologic regime with extended intermittent period altered the riparian forests to become less suitable for native plants that adapt to a mesic environment, allowing the gaps previously occupied by the natives to be readily invaded by drought-tolerant alien species.

Our results provide several important implications for urban planners and ecosystem managers. First, mechanical removal will not eliminate alien species from urban riparian forests. An empty space created by the removal would be quickly refilled by fast growing and disturbance-tolerant alien invaders as long as severe disturbances are continued. This leads to a corollary of the first implication: the remedy should come from a watershed-wide managerial scheme. Several municipalities have adopted stormwater management schemes, such as low impact development, to mitigate hydrologic alteration by development. However, the current management schemes focus mainly on flood control but often overlook the overall hydrologic cycle of a watershed, particularly their effects on baseflow during periods without rainfall. For instance, a detention/retention basin, the most commonly used stormwater best management practice designed to reduce peak discharge by retaining water during storm events, does not necessarily maintain groundwater level unless they are carefully placed by taking into account local infiltration capacity. Many of these basins are even lined with impermeable materials for easy maintenance. The retained stormwater will quickly evaporate instead of infiltrate, especially in hot and semi-arid region like Austin and could further aggravate the drought, through decreased baseflow, in downstream ecosystems. We recommend that urban planners and ecosystem managers take a holistic approach to protect valuable riparian forests from the invasion of alien species.

CHAPTER V

CONCLUSIONS

Biological invasion has received attentions due to a concern for loss of biodiversity (Kendle and Rose, 2000). This study showed that urban riparian forests are more invaded by alien species than rural ones. Hydrologic disturbance appears to be an underlying cause of the increased invasibility in urban riparian forests. Nonmetric multidimensional scaling (NMDS) suggested that environmental conditions in the study forests can be described by five dimensions. The degree of watershed urbanization covaried with a dimension that represents the disturbance regime of riparian forests. Multivariate regression analysis showed that, among the five NMDS dimensions, only this dimension significantly affected the degree of invasibility in the riparian forest. Considering that this dimension consists of other variables, such as the degree of stream dryness and canopy gap percentage, I concluded that watershed urbanization facilitated the alien invasion through increasing disturbance levels.

In chapter III, I showed that urbanization did not necessarily increase peakflow of the study streams. I found that peakflow increases only in gentle slope watersheds during the last two decades when rapid urbanization occurred in the study area. In hillslope watersheds, however, urbanization even decreased peakflow. I attributed the decreased peakflow in hillslope watersheds to a stair-stepped landscape formed by heavy earthwork during construction. The stair-stepped landscape slowed down stormwater runoff and consequently increased the travel time to downstream. Unlike the contrasting

pattern of peakflow, baseflows decreased in all the study area during the last two decades. Combining the findings in Chapter III and Chapter IV, I concluded that a dominant type of disturbance that led to the biological invasion to urban riparian forests were drought rather than floods in a hot and semi-arid climatic region.

Chapter II presents the method of measuring the degrees of watershed urbanization using Landsat TM images. I showed that support vector machine (SVM) with pairwise coupling was superior to other methods in subpixel impervious surface mapping. A winter image was more suited to urban land cover mapping because there was less tree canopy hiding impervious surface.

The results of this study provide several recommendations for urban planners and policy makers.

First, planners should establish a development plan by adapting natural topography. As discussed in Chapter III, landform grading that creates stair-stepped landforms in a hillslope watershed reduces surface runoff. This also leads to fast recession in streamflow. Urbanization could degrade the ecosystem service supplied by this ecosystem because the stream dryness severely disturbs a riparian forest in hot and semi-arid climate. I recommend that planners adapt natural topography and avoid a site layout that requires heavy earthworks with cutting and filling the natural slope.

Second, planners should take into account local infiltration capacity when they establish a stormwater management plan. Current stormwater management schemes focus mainly on flood mitigation. One may think that a site plan that mitigates floods also guarantees to infiltrate stormwater into groundwater. However, it is not necessarily

true if a watershed is less permeable, e.g., a watershed with impermeable bedrock near surface. In a less permeable watershed, stormwater best management practices (BMPs), such as detention/retention basins, still effectively mitigate floods, but may not help stormwater infiltration. The stormwater BMPs even worsen drought stress in downstream ecosystem in a case that the retained stormwater evapotranspired back to the atmosphere after the storms. Therefore, planners should carefully establish stormwater management plan by looking into local hydrogeologic conditions so that the site maintains the predevelopment infiltration rate.

Finally, protection of urban riparian forests should be based on a watershed-scale management plan. A site-level management will not mitigate the invasion of alien species in an urban riparian forest. For instance, the direct removal of alien species will not prevent the biological invasion in riparian forests. Unless disturbance levels are alleviated, the alien species will quickly reestablish in the riparian forests after the removal. A comprehensive management plan is required to minimize the hydrologic disturbance resulting from watershed urbanization.

In this study, I provided several recommendations to urban planners and ecosystem managers. Readers should be noted that none of the above recommendations opposes current stormwater management schemes, such as low impact development. In fact, most recommendations share the same principles with the current schemes. Rather, the problem lies on lack of tool to implement these principles. Researchers and practitioners should elaborate planning methods to effectively implement these principles in practice.

REFERENCES

Aguiar, F.C., Ferreira, M.T., 2005. Human-disturbed landscapes: effects on composition and integrity of riparian woody vegetation in the Tagus River basin, Portugal. Environ. Conserv. 32, 30-41.

Alberti, M., Booth, D., Hill, K., Coburn, B., Avolio, C., Coe, S., Spirandelli, D., 2007. The impact of urban patterns on aquatic ecosystems: an empirical analysis in Puget lowland sub-basins. Landscape Urban Plan. 80, 345-361.

Alberti, M., Weeks, R., Coe, S., 2004. Urban land-cover change analysis in central Puget Sound. Photogramm. Eng. Rem. S. 70, 1043-1052.

Arnold, Jr., C.L., Gibbons, C.J., 1996. Impervious surface coverage: the emergence of a key environmental indicator. J. Am. Plann. Assoc. 62, 243-258.

Barrett, M.E., Irish, L.B., Jr., Malina J.F., Jr., Charbeneau, R.J., 1998. Characterization of highway runoff in Austin, Texas, area. J. Environ. Eng.-ASCE 124, 131-137.

Basnyat, P., Teeter, L., Lockaby, B.G., Flynn, K.M., 2000. Land use characteristics and water quality: a methodology for valuing of forested buffers. Environ. Manage. 26, 153-161.

Beeson, C.E., Doyle, P.F., 1995. Comparison of bank erosion at vegetated and non-vegetated channel bends. Water Resour. Bull. 31, 983-990.

Bendix, J., Hupp, C.R., 2000. Hydrological and geomorphological impacts on riparian plant communities. Hydrol. Process 14, 2977-2990.

Booth, D.B., Hartley, D., Jackson, R., 2002. Forest cover, impervious-surface area, and the mitigation of stormwater impacts. J. Am. Water Resour. As. 38, 835-845.

Booth, D.B., Karr, J.R., Schauman, S., Konrad, C.P., Morley, S.A., Larson, M.G., Burges, S.J., 2004. Reviving urban streams: land use, hydrology, biology, and human behavior. J. Am. Water Resour. As. 40, 1351-1364.

Bowles, D.E., Arsuffi, T.L., 1993. Karst aquatic ecosystems of the Edwards Plateau region of central Texas, USA: a consideration of their importance, threats to their existence, and efforts for their conservation. Aquat. Conserv. 3, 317-329.

Box, G.E.P., Jenkins, G.M., 1976. Time Series Analysis: Forecasting and Control, Holden-Day, Oakland, CA.

Brabec, E., Schulte, S., Richards, P.L., 2002. Impervious surfaces and water quality: a review of current literature and its implications for watershed planning. J. Plan. Lit 16, 499-514.

Brandes, D., Cavallo, G.J., Nilson, M.L., 2005. Base flow trends in urbanizing watersheds of the Delaware River basin. J. Am. Water Resour. As. 41, 1377-1391.

Brezonik, P.L., Stadelmann, T.H., 2002. Analysis and predictive models of stormwater runoff volumes, loads, and pollutant concentrations from watersheds in the Twin Cities metropolitan area, Minnesota, USA. Water Res. 36, 1743-1757.

Brinson, M.M., Lugo, A.E., Brown, S., 1981. Primary productivity, decomposition and consumer activity in freshwater wetlands. Annu. Rev. Ecol. Syst. 12, 123-161.

Burges, C.J.C., 1998. A tutorial on support vector machines for pattern recognition. Data Min. Knowl. Disc. 2, 121-167.

Burges, S.J., Wigmosta, M.S., Meena, J.M., 1998. Hydrological effects of land-use change in a zero-order catchment. J. Hydrol. Eng. 3, 86-97.

Burns, D., Vitvar, T., McDonnell, J., Hassett, J., Duncan, J., Kendall, C., 2005. Effects of suburban development on runoff generation in the Croton River basin, New York, USA. J. Hydrol 311, 266-281.

Burton, M.L., Samuelson, L.J., 2008. Influence of urbanization on riparian forest diversity and structure in the Georgia Piedmont, US. Plant Ecol. 195, 99-115.

Burton, M.L., Samuelson, L.J., Mackenzie, M.D., 2009. Riparian woody plant traits across an urban-rural land use gradient and implications for watershed function with urbanization. Landscape Urban Plan. 90, 42-55.

Burton, M.L., Samuelson, L.J., Pan, S., 2005. Riparian woody plant diversity and forest structure along an urban-rural gradient. Urban Ecosyst. 8, 93-106.

Canty, A., Ripley, B., 2009. Package 'boot' (accessed on December 9, 2009). http://cran.r-project.org/web/packages/boot/boot.pdf.

Caratti, J.F., 2006. Line Intercept (LI), in: *FIREMON: Fire effects monitoring and inventory system* (D.C. Lutes, ed.), Rocky Mountain Research Station, Natural Resources Research Center, Fort Collins, CO.

Chin, A., Gregory, K.J., 2001. Urbanization and adjustment of ephemeral stream

channels. Ann. Assoc. Am. Geogr. 91, 595-608.

City of Austin, 2008. Watershed Ordinances: A Retrospective (accessed on September 16, 2008). http://www.ci.austin.tx.us/watershed/ordinances.htm.

Cooper, D.J., Andersen, D.C., Chimner, R.A., 2003. Multiple pathways for woody plant establishment on floodplains at local to regional scales. J. Ecol. 91, 182-196.

Corbacho, C., Sánchez, J.M., Costillo, E., 2003. Patterns of structural complexity and human disturbance of riparian vegetation in agricultural landscapes of a Mediterranean area. Agr. Ecosyst. Environ. 95, 495-507.

Cronk, J.K., Fennessy, M.S., 2001. Wetland Plants: Biology and Ecology, Lewis Publishers, Boca Raton, FL.

Dietz, M.E., Clausen, J.C., 2008. Stormwater runoff and export changes with development in a traditional and low impact subdivision. J. Environ. Manage. 87, 560-566.

Dimitriadou, E., Hornik, K., Leisch, F., Meyer, D., Weingessel, A., 2009. Package 'e1071' (accessed on November 9, 2009). http://cran.r-project.org/web/packages/e1071/e1071.pdf.

Elton, C.S., 1958. The Ecology of Invasions by Animals and Plants, Methuen & Company, London.

Everitt, B., 2005. An R and S-Plus Companion to Multivariate Analysis, Springer, London.

Farahmand, T., Fleming, S.W., 2007. Detection and visualization of storm hydrograph changes under urbanization: an impulse response approach. J. Environ. Manage. 85, 93-100.

Fisher, P.F., Pathirana, S., 1990. The evaluation of fuzzy membership of land cover classes in the suburban zone. Remote Sens. Environ. 34, 121-132.

Foody, G.M., Mathur, A., 2004. Toward intelligent training of supervised image classifications: directing training data acquisition for SVM classification. Remote Sens. Environ. 93, 107-117.

Foody, G.M., Mathur, A., 2006. The use of small training sets containing mixed pixels for accurate hard image classification: training on mixed spectral responses for classification by a SVM. Remote Sens. Environ. 103, 179-189.

Gillies, R.R., Box, J.B., Symanzik, J., Rodemaker, E.J., 2003. Effects of urbanization on the aquatic fauna of the Line Creek watersheds, Atlanta - a satellite perspective. Remote Sens. Environ. 86, 411-422.

Glenn, E.P., Nagler, P.L., 2005. Comparative ecophysiology of *Tamarix ramosissima* and native trees in western U.S. riparian zones. J. Arid Environ. 61, 419-446.

Goonetilleke, A., Thomas, E., Ginn, S., Gilbert, D., 2005. Understanding the role of land use in urban stormwater quality management. J. Environ. Manage. 74, 31-42.

Greer, K., Stow, D., 2003. Vegetation type conversion in Los Peñasquitos Lagoon, California: an examination of the role of watershed urbanization. Environ. Manage. 31, 489-503.

Groffman, P.M., Bain, D.J., Band, L.E., Belt, K.T., Brush, G.S., Grove, J.M., Pouyat, R.V., Yesilonis, I.C., Zipperer, W.C., 2003. Down by the riverside: urban riparian ecology. Front. Ecol. Environ. 1, 315-321.

Groffman, P.M., Boulware, N.J., Zipperer, W.C., Pouyat, R.V., Band, L.E., Colosimo, M.F., 2002. Soil nitrogen cycle processes in urban riparian zones. Environ. Sci. Technol. 36, 4547-4552.

Hastie, T., Tibshirani, R., 1998. Classification by pairwise coupling. Ann. Stat. 26, 451-471.

Hatt, B.E., Fletcher, T.D., Walsh, C.J., Taylor, S.L., 2004. The influence of urban density and drainage infrastructure on the concentrations and loads of pollutants in small streams. Environ. Manage. 34, 112-124.

Hession, W.C., Pizzuto, J.E., Johnson, T.E., Horwitz, R.J., 2003. Influence of bank vegetation on channel morphology in rural and urban watersheds. Geology 31, 147-150.

Hollis, G.E., 1975. The effect of urbanization on floods of different recurrence interval. Water Resour. Res. 11, 431-435.

Hood, M.J., Clausen, J.C., Warner, G.S., 2007. Comparison of stormwater lag times for low impact and traditional residential development. J. Am. Water Resour. As. 43, 1036-1046.

Hood, W.G., Naiman, R.J., 2000. Vulnerability of riparian zones to invasion by exotic vascular plants. Plant Ecol. 148, 105-114.

Horton, J.L., Clark, J.L., 2001. Water table decline alters growth and survival of *Salix*

gooddingii and *Tamarix chinensis* seedlings. Forest Ecol. Manag. 140, 239-247.

Hu, X., Weng, Q., 2009. Estimating impervious surfaces from medium spatial resolution imagery using the self-organizing map and multi-layer perceptron neural networks. Remote Sens. Environ. 113, 2089-2102.

Huang, C., Townshend, J.R.G., 2003. A stepwise regression tree for nonlinear approximation: applications to estimating subpixel land cover. Int. J. Remote Sens. 24, 75-90.

ITT Visual Information Solutions, 2008. ENVI Tutorials (accessed on February 21, 2008). http://www.ittvis.com/ProductServices/ENVI/Tutorials.aspx.

Jennings, D.B., Jarnagin, S.T., 2002. Changes in anthropogenic impervious surfaces, precipitation and daily streamflow discharge: a historical perspective in a mid-Atlantic subwatershed. Landscape Ecol. 17, 471-489.

Jones, J.A., Swanson, F.J., Wemple, B.C., Snyder, K.U., 2000. Effects of roads on hydrology, geomorphology, and disturbance patches in stream networks. Conserv. Biol. 14, 76-85.

Kendle, A.D., Rose, J.E., 2000. The aliens have landed! What are the justifications for 'native only' policies in landscape plantings? Landscape Urban Plan. 47, 19-31.

Kim, Y., Engel, B.A., Lim, K.J., Larson, V., Duncan, B., 2002. Runoff impacts of land-use change in Indian River Lagoon watershed. J. Hydrol. Eng. 7.

King, S.A., Buckney, R.T., 2000. Urbanization and exotic plants in northern Sydney streams. Austral Ecol. 25, 455-461.

Lardeux, C., Frison, P.-L., Tison, C., Souyris, J.-C., Stoll, B., Frumeau, B., Rudant, J.-P., 2009. Support vector machine for multifrequency SAR polarimetric data classification. IEEE T. Geosci. Remote 47, 4143-4152.

Lee, J.G., Heaney, J.P., 2003. Estimation of urban imperviousness and its impacts on storm water systems. J. Water Res. Pl.-ASCE 129, 419-426.

Lee, S., Lathrop, R.G., 2006. Subpixel analysis of Landsat ETM+ using self-organizing map (SOM) neural networks for urban land cover characterization. IEEE T. Geosci. Remote 44, 1642-1654.

Leopold, L.B., 1968. Hydrology for Urban Land Planning-A Guidebook on the Hydrologic Effects of Urban Land Use, U.S. Department of Interior, Washington, DC.

Levine, J.M., 2000. Species diversity and biological invasions: relating local process to community pattern. Science 288, 852-854.

Li, M.-H., Barrett, M.E., Rammonhan, P., Olivera, F., Landphair, H.C., 2008. Documenting stormwater quality on Texas highways and adjacent vegetated roadsides. J. Environ. Eng.-ASCE 134, 48-59.

Limas, M.C., Meré, J.B.O., González, V., Ascacibar, F.J.M.d.P., Espinoza, A.V.P., Elías, F.A., 2009. Package 'AMORE' (accessed on October 17, 2009). http://cran-r-project.org/web/packages/AMORE/AMORE.pdf.

Liu, D., Kelly, M., Gong, P., 2006. A spatial-temporal approach to monitoring forest disease spread using multi-temporal high spatial resolution imagery. Remote Sens. Environ. 101, 167-180.

Liu, W., Wu, E.Y., 2005. Comparison of non-linear mixture models: sub-pixel classification. Remote Sens. Environ. 94, 145-154.

Lu, D., Weng, Q., 2004. Spectral mixture analysis of the urban landscape in Indianapolis with Landsat ETM+ imagery. Photogramm. Eng. Rem. S. 70, 1053-1062.

Lytle, D.A., Merritt, D.M., 2004. Hydrologic regimes and riparian forests: a structured population model for cottonwood. Ecology 85, 2493-2503.

Magee, T.K., Ringold, P.L., Bollman, M.A., 2008. Alien species importance in native vegetation along wadeable streams, John Day River basin, Oregon, USA. Plant Ecol. 195, 287-307.

Magurran, A.E., 1988. Ecological Diversity and Its Measurement, Princeton University Press, Princeton, NJ.

Marsh, W.M., Marsh, N.L., 1995. Hydrogeomorphic considerations in development planning and stormwater management, Central Texas Hill Country, USA. Environ. Manage. 19, 693-702.

Maskell, L.C., Bullock, J.M., Smart, S.M., Thompson, K., Hulme, P.E., 2006. The distribution and habitat associations of non-native plant species in urban riparian habitats. J. Veg. Sci. 17, 499-508.

Mazzoni, D., Logan, J.A., Diner, D., Kahn, R., Tong, L., Li, Q., 2007. A data-mining approach to associating MISR smoke plume heights with MODIS fire measurements. Remote Sens. Environ. 107, 134-148.

McMahan, C.A., Frye, R.G., Brown, K.L., 1984. The Vegetation Types of Texas Including Cropland, Wildlife Division, Texas Parks and Wildlife Department, Austin, TX.

Medina, A.L., 1990. Possible effects of residential development on streamflow, riparian plant communities, and fisheries on small mountain streams in central Arizona. Forest Ecol. Manag. 33/34, 351-361.

Melgani, F., Bruzzone, L., 2004. Classification of hyperspectral remote sensing images with support vector machines. IEEE T. Geosci. Remote 42, 1778-1790.

Meyer, S.C., 2005. Analysis of base flow trends in urban streams, northeastern Illinois, USA. Hydrogeol. J. 13, 871-885.

Mitsch, W.J., Gosselink, J.G., 2007. Wetlands, John Wiley & Sons, Hoboken, NJ.

Mitsch, W.J., Horne, A.J., Nairn, R.W., 2000. Nitrogen and phosphorus retention in wetlands- ecological approaches to solving excess nutrient problems. Ecol. Eng. 14, 1-7.

Moffatt, S.F., McLachlan, S.M., Kenkel, N.C., 2004. Impacts of land use on riparian forest along an urban-rural gradient in southern Manitoba. Plant Ecol. 174, 119-135.

Moggridge, H.L., Gurnell, A.M., Mountford, J.O., 2009. Propagule input, transport and deposition in riparian environments: the importance of connectivity for diversity. J. Veg. Sci. 20, 465-474.

Moody, A., Gopal, S., Strahler, A.H., 1996. Artificial neural network response to mixed pixels in coarse-resolution satellite data. Remote Sens. Environ. 58, 329-343.

Morris, L.L., Walck, J.L., Hidayati, S.N., 2002. Growth and reproduction of the invasive *Ligustrum sinense* and native *Forestiera ligustrina* (Oleaceae): implications for the invasion and persistence of a nonnative shrub. Int. J. Plant Sci. 163, 1001-1010.

Morse, C.C., Huryn, A.D., Cronan, C., 2003. Impervious surface area as a predictor of the effects of urbanization on stream insect communities in Maine, U.S.A. Environ. Monit. Assess. 89, 95-127.

Nash, N.E., Sutcliffe, J.V., 1970. River flow forecasting through conceptual models part I - a discussion of principles. J. Hydrol. 10, 282-290.

Nemmour, H., Chibani, Y., 2006. Multiple support vector machines for land cover

change detection: an application for mapping urban extensions. ISPRS J. Photogramm 61, 125-133.

Nilsson, C., Jansson, R., Zinko, U., 1997. Long-term responses of river-margin vegetation to water-level regulation. Science 276, 798-800.

O'Connell, P.E., Clarke, R.T., 1981. Adaptive hydrological forecasting - a review. Hydrol. Sci. Bull. 26, 179-205.

Oksanen, J., Kindt, R., Legendre, P., O'Hara, B., Simpson, G.L., Solymos, P., Stevens, M.H.H., Wagner, H., 2009. Package 'vegan' (accessed on November 3, 2009). URL: http://cran.r-project.org/web/packages/vegan/vegan.pdf.

Oneal, A.S., Rotenberry, J.T., 2008. Riparian plant composition in an urbanizing landscape in southern California, U.S.A. Landscape Ecol. 2008, 553-567.

Pal, M., Mather, P.M., 2004. Assessment of the effectiveness of support vector machines for hyperspectral data. Future Gener. Comp. Sy. 20, 1215-1225.

Pettit, N.E., Froend, R.H., 2001. Variability in flood disturbance and the impact on riparian tree recruitment in two contrasting river systems. Wetlands Ecol. Manag. 9, 13-25.

Pinay, G., Ruffinoni, C., Fabre, A., 1995. Nitrogen cycling in two riparian forest soils under different geomorphic conditions. Biogeochemistry 30, 9-29.

Planty-Tabacchi, A.-M., Tabacchi, E., Naiman, R.J., Deferrari, C., Décamps, H., 1995. Invasibility of species-rich communities in riparian zones. Conserv. Biol. 10, 598-607.

Pratt, R.B., Black, R.A., 2006. Do invasive trees have a hydraulic advantage over native trees? Biol. Invasions 8, 1331-1341.

Ridd, M.K., 1995. Exploring a V-I-S (vegetation-impervious surface-soil) model for urban ecosystem analysis through remote sensing: a comparative anatomy for cities. Int. J. Remote Sens. 16, 2165-2185.

Riley, S.P.D., Busteed, G.T., Kats, L.B., Vandergon, T.L., Lee, L.F.S., Dagit, R.G., Kerby, J.L., Fisher, R.N., Sauvajor, R.M., 2005. Effects of urbanization on the distribution and abundance of amphibians and invasive species in southern California streams. Conserv. Biol. 19, 1894-1907.

Rogers, G.O., DeFee II, B.B., 2005. Long-term impact of development on a watershed: early indicators of future problems. Landscape Urban Plan. 73, 215-233.

Rose, S., Peters, N.E., 2001. Effects of urbanization on streamflow in the Atlanta area (Georgia, USA): a comparative hydrological approach. Hydrol. Process 15, 1441-1457.

Roy, A.H., Shuster, W.D., 2009. Assessing impervious surface connectivity and applications for watershed management. J. AM. Water Resour. As. 45, 198-209.

Salas, J.D., Tabios III, G.Q., Bartolini, P., 1985. Approaches to multivariate modeling of water resources time series. Water Resour. Bull. 21, 683-708.

SAS Institute Inc., 2004. SAS 9.1 Help and Documentation, SAS Institute Inc., Cary, NC.

Scanlon, B.R., Mace, R.E., Barrett, M.E., Smith, B., 2003. Can we simulate regional groundwater flow in a karst system using equivalent porous media models? case study, Barton Springs Edwards aquifer, USA. J. Hydrol. 276, 137-158.

Schoonover, J.E., Lockaby, B.G., Pan, S., 2005. Changes in chemical and physical properties of stream water across an urban-rural gradient in western Georgia. Urban Ecosyst. 8, 107-124.

Shafroth, P.B., Stromberg, J.C., Patten, D.T., 2002. Riparian vegetation response to altered disturbance and stress regimes. Ecol. Appl. 12, 107-123.

Simmons, D.L., Reynolds, R.J., 1982. Effects of urbanization on base flow of selected south-shore streams, Long Island, New York. Water Resour. Bull. 18, 797-805.

Small, C., 2001. Estimation of urban vegetation abundance by spectral mixture analysis. Int. J. Remote Sens. 22, 1305-1334.

Small, C., 2002. Multitemporal analysis of urban reflectance. Remote Sens. Environ. 81, 427-442.

Snyder, K.A., Williams, D.G., 2000. Water sources used by riparian trees varies among stream types on the San Pedro River, Arizona. Agr. Forest Meteorol. 105, 227-240.

Soil Conservation Service, 1974. Soil Survey of Travis County, Texas, U.S. Department of Agriculture, Washington, DC.

Stohlgren, T.J., Binkley, D., Chong, G.W., Kalkhan, M.A., Schell, L.D., Bull, K.A., Otsuki, Y., Newman, G., Bashkin, M., Son, Y., 1999. Exotic plant species invade hot spots of native plant diversity. Ecol. Monogr. 69, 25-46.

Stohlgren, T.J., Bull, K.A., Otsuki, Y., Villa, C.A., Lee, M., 1998. Riparian zones as havens for exotic plant species in the central grasslands. Plant Ecol. 138, 113-125.

Stromberg, J., 1998. Dynamics of Fremont cottonwood (*Populus fremontii*) and saltcedar (*Tamarix chinensis*) populations along the San Pedro River, Arizona. J. Arid Environ. 40, 133-155.

Stromberg, J.C., Beauchamp, V.B., Dixon, M.D., Lite, S.J., Paradzick, C., 2007. Importance of low-flow and high-flow characteristics to restoration of riparian vegetation along rivers in arid south-western United States. Freshwater Biol. 52, 651-679.

Su, L., Chopping, M.J., Rango, A., Martonchik, J.V., Peters, D.P.C., 2007. Support vector machines for recognition of semi-arid vegetation types using MISR multi-angle imagery. Remote Sens. Environ. 107, 299-311.

Sutherland, A.B., Meyer, J.L., Gardiner, E.P., 2002. Effects of land cover on sediment regime and fish assemblage structure in four southern Appalachian streams. Freshwater Biol. 47, 1791-1805.

Tickner, D.P., Angold, P.G., Gurnell, A.M., Mountford, J.O., 2001. Riparian plant invasions: hydrogeomorphological control and ecological impacts. Prog. Phys. Geog. 25, 22-52.

U.S. Census Bureau, 2009. Population Finder: Austin City, Texas (accessed on July 15, 2009). http://factfinder.census.gov.

U.S. Environmental Protection Agency, 2000. Low Impact Development (LID): A Literature Review, Washington DC.

U.S. National Climatic Data Center, 2009. NCDC: Locate Weather Observation Station Record (accessed on September 6, 2009). http://www4.ncdc.noaa.gov/cgi-win/wwcgi.dll?wwDI~StnSrch~StnID~20024676.

von Holle, B., 2005. Biotic resistance to invader establishment of a southern Appalachian plant community is determined by environmental conditions. J. Ecol. 93, 16-26.

Walsh, C.J., Roy, A.H., Feminella, J.W., Cottingham, P.D., Groffman, P.M., Morgan, R.P., II, 2005. The urban stream syndrome: current knowledge and the search for a cure. J. N. Am. Benthol. Soc. 24, 706-723.

Walton, J.T., 2008. Subpixel urban land cover estimation: comparing cubist, random forests, and support vector regression. Photogramm. Eng. Rem. S. 74, 1213-1222.

Wang, L., John, L., Kanehl, P., Bannerman, R., 2001. Impacts of urbanization on stream habitat and fish across multiple spatial scales. Environ. Manage. 28, 255-266.

Watts, S.H., Seitzinger, S.P., 2000. Denitrification rates in organic and mineral soils from riparian sites: a comparison of N_2 flux and acetylene inhibition methods. Soil. Biol. Biochem. 32, 1383-1392.

Weng, Q., Hu, X., 2008. Medium spatial resolution satellite imagery for estimating and mapping urban impervious surfaces using LSMA and ANN. IEEE T. Geosci. Remote 46, 2397-2406.

White, M.D., Greer, K.A., 2006. The effects of watershed urbanization on the stream hydrology and riparian vegetation of Los Peñasquitos Creek, California. Landscape Urban Plan. 74, 125-138.

Wilcox, B.P., Taucer, P.I., Munster, C.L., Owens, M.K., Mohanty, B.P., Sorenson, J.R., Bazan, R., 2008. Subsurface stormflow is important in semiarid karst shrublands. Geophys. Res. Lett. 35, L10403.

Woodruff, Jr, C.M., Wilding, L.P., 2008. Bedrock, soils, and hillslope hydrology in the Central Texas Hill Country, USA: implications on environmental management in a carbonate-rock terrain. Environ. Geol. 55, 605-618.

Wu, C., Murray, A.T., 2003. Estimating impervious surface distribution by spectral mixture analysis. Remote Sens. Environ. 84, 493-505.

Wu, T.-F., Lin, C.-J., Weng, R.C., 2004. Probability estimates for multi-class classification by pairwise coupling. J. Mach. Learn. Res. 5, 979-1005.

Young, P., 2003. Top-down and data-based mechanistic modelling of rainfall-flow dynamics at the catchment scale. Hydrol. Process 17, 2195-2217.

Zedler, J.B., Kercher, S., 2004. Causes and consequences of invasive plants in wetlands: opportunities, opportunists, and outcomes. Crit. Rev. Plant Sci. 23, 431-452.

VITA

Chan Yong Sung received his Bachelor of Engineering degree in urban planning from Hongik University in 1999, and a Master of Engineering degree in urban planning from Hongik University in 2001. He received a joint degree of Master of Public Affairs and Master of Environmental Science from Indiana University at Bloomington in 2004. He received a Ph.D. degree in urban and regional sciences at Texas A&M University in 2010. His research interest is multidisciplinary and covers various topics related to urban environments such as environmental planning and policy, urban ecosystem management, and water resources protection.

Chan Yong Sung may be reached at 3137 TAMU, College Station, TX 77843. His email is cysung@gmail.com.